International Journal for Parasitology 45 (2015) 1–16

Contents lists available at ScienceDirect

International Journal for Parasitology

journal homepage: www.elsevier.com/locate/ijpara

Morphology and phylogeny of *Agmasoma penaei* (Microsporidia) from the type host, *Litopenaeus setiferus*, and the type locality, Louisiana, USA ☆

Yuliya Sokolova [a,b,*], Adrian Pelin [c], John Hawke [d], Nicolas Corradi [c]

[a] Department of Comparative Biomedical Studies, School of Veterinary Medicine, Louisiana State University, Baton Rouge, LA, USA
[b] Institute of Cytology, Russian Academy of Sciences, St. Petersburg, Russia
[c] Canadian Institute for Advanced Research, Department of Biology, University of Ottawa, Ottawa, ON K1N 6N5, Canada
[d] Department of Pathobiological Sciences, School of Veterinary Medicine, Louisiana State University, Baton Rouge, LA, USA

ARTICLE INFO

Article history:
Received 3 June 2014
Received in revised form 15 July 2014
Accepted 16 July 2014
Available online 18 October 2014

Keywords:
Microsporidia
Decapoda
Agmasoma penaei
Litopenaeus setiferus
Louisiana
Electron microscopy
Molecular taxonomy

ABSTRACT

Since June 2012, samples of wild caught white shrimp, *Litopenaeus setiferus,* from the Gulf of Mexico, Plaquemines and Jefferson Parishes (Louisiana, USA) with clinical signs of microsporidiosis have been delivered to the Louisiana Aquatic Diagnostic Laboratory for identification. Infection was limited predominantly to female gonads and was caused by a microsporidium producing roundish pansporoblasts with eight spores (3.6 × 2.1 μm) and an anisofilar (2–3 + 4–6) polar filament. These features allowed identification of the microsporidium as *Agmasoma penaei* Sprague, 1950. *Agmasoma penaei* is known as a microsporidium with world-wide distribution, causing devastating epizootic disease among wild and cultured shrimps. This paper provides molecular and morphological characterisation of *A. penaei* from the type host and type locality. Comparison of the novel ssrDNA sequence of *A. penaei* from Louisiana, USA with that of *A. penaei* from Thailand revealed 95% similarity, which suggests these geographical isolates are two different species. The *A. penaei* sequences did not show significant homology to any other examined taxon. Phylogenetic reconstructions using the ssrDNA and alpha- and beta-tubulin sequences supported its affiliation with the Clade IV Terresporidia sensu Vossbrink 2005, and its association with parasites of fresh and salt water crustaceans of the genera *Artemia*, *Daphnia* and *Cyclops*.

1. Introduction

Microsporidiosis is the most common and harmful disease of decapods (phylum Arthropoda: class Crustacea: order Decapoda) caused by eukaryotic microbes (Overstreet, 1973; Kelly, 1979; Johnson, 1995; Morado, 2011). Microsporidial infections caused by more than 20 species belonging to 17 genera have been reported from a variety of decapod species belonging to the family Penaeidae, suborder Dendrobranchiata, as well as four infraorders of the suborder Pleocyemata, namely, Caridea, Astacidea, Brachiura and Anomura (Canning et al., 2002; Stentiford et al., 2013b, 2014). Microsporidiosis in decapods is often linked with reduced host fecundity, elevated susceptibility to predators and to other diseases, and sensitivity to unfavorable environmental conditions (Hutton et al., 1959).

Since June 2012, samples of wild *Litopenaeus setiferus* (Latin names of penaeids from this point forward adhere to taxonomy according to Perez Farfante (1997)) from Plaquemines and Jefferson Parishes (Louisiana (LA), USA) fisheries with clinical signs of microsporidiosis (white tumour-like growths within and below the carapace) were delivered to the Louisiana Aquatic Diagnostic Laboratory on four occasions for further examination. The shrimp were collected by commercial trawlers working in the areas of Bay Jimmy and Barataria Bay. Light (LM) and electron microscopy (EM) examination indicated the infection was caused by a microsporidium producing octets of spores in sub-persistent roundish sporophorous vesicles (SVs). The microsporidium was readily identified as *Agmasoma penaei* based on morphological characters, geographical locality, host species and tissue tropism. This species, formerly known as *Thelohania penaei* Sprague 1950, was later transferred from the genus *Thelohania* to a newly erected

☆ *Note:* Nucleotide sequence data reported in this paper are available in the GenBank database under accession numbers KF549987, PRJNA206557, KJ579182, KJ579183.

* Corresponding author at: Microscopy Center, Department of Comparative Biological Sciences, School of Veterinary Medicine, Louisiana State University, 1909 Skip Bertman Drive, Baton Rouge, LA 70803, USA. Tel./fax: +1 225 5789899.
E-mail address: sokolova@lsu.edu (Y. Sokolova).

http://dx.doi.org/10.1016/j.ijpara.2014.07.013
0020-7519/

monotypic genus, *Agmasoma,* by Hazard and Oldacre in 1976 in their revision of the genus *Thelohania* (Sprague, 1950; Hazard and Oldacre, 1975).

Agmasoma penaei has been known to cause "cotton disease" in White Atlantic shrimp, *L. setiferus*, since 1920 (Viosca, 1945; Miglarese and Shealy, 1974). It has been recorded in eight species of penaeid shrimp (Table 1), and has been shown to adversely affect commercial shrimp fisheries and shrimp aquaculture worldwide (Sprague and Cough, 1971; Sprague, 1977; Kelly, 1979; Flegel et al., 1992; Clotilde-Ba and Toguebaye, 1994, 2001; Vidal-Martínez et al., 2002; Toubiana et al., 2004; Laisutisan et al., 2009).

In the Gulf of Mexico, the most severe epizootic of microsporidiosis among white shrimp *L. setiferus* due to *A. penaei* was recorded in 1929. It resulted in an infection prevalence of 90%, mass mortality, loss of 99% of egg production and an unprofitable fishery industry for several years (Gunter, 1967; Muncy, 1984). Except for epizootic peaks, the infection rate of this parasite in wild populations of white shrimp in the Gulf of Mexico normally does not exceed 1% (Lightner, 1996). During the last 2 years, the reports of microsporidian infections in areas of the Gulf of Mexico have increased, particularly in locations adjacent to the Deepwater Horizon oil spill (J. Hawke, unpublished observations and conversations with local marine biologists and agents)).

Three geographical isolates parasitising three different penaeid hosts from different geographic locations, were examined ultrastructurally. These are: the Louisiana isolate from Atlantic white shrimp, *L. setiferus* (Hazard and Oldacre, 1975), the Senegal isolate from the Southern pink shrimp, *Farfantepenaus notialis* (Clotilde-Ba and Toguebaye, 1994), and the Thailand isolate from Pacific white shrimp, *Litopenaeus vannamei* (Laisutisan et al., 2009). All three isolates displayed a similar pattern of octosporous sporogony, pyriform shape of spores and spore ultrastructure with conspicuous anisofilar polar filaments. Prior to this study, data on fine morphology of the Louisiana isolate was limited to two EM images (Hazard and Oldacre, 1975). The Senegal and Thailand isolates of *A. penaei* have been studied more thoroughly, however the ultrastructure of the organism has not been described sufficiently. Data on pathogenicity, tissue tropism, transmission and sexuality are scarce and controversial among these three and other geographical isolates of *A. penaei* (Table 1). Only one *A. penaei* isolate parasitising cultured *Fenneropenaeus merguiensis* and *Penaeus monodon* in Thailand has been characterised using molecular tools and a fragment of its ssrDNA sequence is available via GenBank (Pasharawipas and Flegel, 1994; Pasharawipas et al., 1994).

The major goal of this paper is to provide morphological and molecular characterisation of *A. penaei* from the type host and type locality, which would serve as an important reference for identification of geographical isolates of this microsporidium. We also comparatively evaluate the fine morphology of three geographical isolates of *A. penaei*, assess relatedness of *A. penaei* from Louisiana to other microsporidia parasitising decapods using ssrDNA-based phylogenetic analysis, and present molecular and phylogenetic comparisons of *A. penaei* genes for ssrRNA and alpha- and beta-tubulins with other microsporidian orthologues available in GenBank.

2. Materials and methods

2.1. Materials

White shrimp, *L. setiferus* Linnaeus 1767, were caught by commercial trawling in the Gulf of Mexico in the bays and offshore from Plaquemines and Jefferson Parishes, Louisiana, USA. An unusually high number of shrimp harbouring macroscopic whitish lesions and tumour-like growths on the carapaces and abdomens were noticed by shrimpers. Thirty shrimps with these clinical signs were delivered to the Louisiana Aquatic Diagnostic Laboratory (Louisiana State University (LSU) School of Veterinary Medicine (SVM), Baton Rouge, LA, USA) from May 2012 to November 2013. In all of the cases, shrimp were caught alive, kept on ice and delivered within 6–24 h after being caught. All delivered shrimp were females, with sizes ranging from 100 to 120 mm for those caught in May, and 130 to 180 mm for those caught later in the year. The material examined in this study included 18 shrimp; two sampled on 16 May 2012 (case LADL12-047); two on 22 May

Table 1
Records of occurrence of *Agmasoma penaei* among penaeid shrimps.

Shrimp species	Locality	Wild/ cultured	Tissues	Techniques	References
Atlantic white shrimp *Litopenaeus setiferus* (Type host)	Gulf of Mexico (LA, MI,FL coast); type locality: around Grand Isle, LA	Wild	Gonads	LM, TEM, SEM, ssrDNA	Sprague (1950) Hazard and Oldacre (1975) This paper
Pacific white shrimp *Litopenaeus vannamei*	Thailand, Indian Ocean	Cultured	Abdominal muscles, hepatopancreas	LEM, TEM	Laisutisan et al. (2009)
Indian prawn *Fenneropenaeus indicus*	Republic of South Africa shore: South Atlantic/Indian Ocean	Wild	Gonads	LM	Sprague and Cough (1971) Sprague (1977)
Banana shrimp *Fenneropenaeus merguiensis*	Thailand, Indian Ocean	Wild Cultured	No data	LM, ssrDNA	Pasharawipas and Flegel (1994) Pasharawipas et al. (1994)
Pink shrimp *Farfantepenaeus duorarum*	Atlantic coast of South Florida	Wild	Muscles, hepatopancreas, gonads	LM	Kelly (1979)
Pink shrimp *Farfantepenaeus notialis*	West African coast of South Atlantic (Senegal)	Wild	Gonads, hepatopancreas, heart, intestine, nervous system, muscle; xenomas	LM, TEM	Clotilde-Ba and Toguebaye (1994)
Black tiger shrimp *Penaeus monodon*	West African coast of South Atlantic (Senegal)	Cultured	Muscles	LM	Clotilde-Ba and Toguebaye (2001)
	West coast of Madagascar	Wild	No data	SEM	Toubiana et al. (2004)
	Thailand, Indian Ocean	Cultured	No data	LM, ssrDNA	Pasharawipas and Flegel (1994), Pasharawipas et al. (1994)
Green tiger prawn *Penaeus semisulcatus*	Thailand, Indian Ocean	Wild	No data	SEM	Toubiana et al. (2004)

LA, Louisiana, USA; MI, Mississippi, USA; FL, Florida, USA; LM, light microscopy; TEM, transmission electron microscopy; SEM, scanning electron microscopy.

2012 (case LADL12-053), eight on 2 October 2012 (case LADL12-113), and six on 11 October 2012 (case LADL12-19). All samples were studied by LM, but only eight by EM.

2.2. Histopathology and analysis of tissue tropism

One to three whole shrimp were injected with 5 ml of Davidson's fixative, placed in fresh Davidson's fixative at approximately 10× their volume for 24 to 48 h and then transferred to 70% ethanol (Bell and Lightner, 1988). Standard histological protocols, based on the procedures of Luna (1968), were employed by the Louisiana Animal Disease Diagnostic Laboratory, Histology Laboratory, LSU SVM. Tissues were manually trimmed to a width of 10 mm, placed in cassettes, processed through an alcohol series and embedded in paraffin in a Tissue Tek VIP 5 (Sakura Finetek USA Inc., Torrance, CA, USA). Tissues were sectioned at a thickness of 5 μm, mounted on glass slides and stained with Hematoxylin-Biebrich scarlet solution (Luna stain). This stain has traditionally been used to stain erythrocytes and eosinophil granules but has recently been shown to selectively stain for microsporidia-infected tissue (Peterson et al., 2011). For observation of microsporidia and ultrastructural studies of the infected tissues, the gonads, hepatopancreas, thoracal and abdominal muscles, subcuticular lesions of the carapace, and intestines were isolated from dissected shrimp. Smears from these tissues were either examined directly under a light microscope with phase contrast optics or were fixed by absolute methanol, stained with Trichrome stain, Calcofluor and Giemsa, as previously described (Sokolova and Fuxa, 2008), and examined with bright field optics. Smears and sections were examined with a Zeiss Axioplan microscope equipped with an Olympus DP73 digital camera, or with a Zeiss Observer Z1 with mosaic tiling function. ImagePro7.0 software was used for spore measurements. For EM, small pieces of infected tissues were fixed in a mixture of 2% paraformaldehyde and 1.25% glutaraldehyde in 0.1 M cacodilate buffer supplemented with 5% sucrose for 2 h, washed several times in the same buffer and post-fixed in 1% osmium for 1 h. All procedures were performed at room temperature. Samples were then thoroughly washed in water and dehydrated in ascending ethanol series and propylene oxide, and embedded in Epon–Araldite. Blocks were sectioned with Ultratome Leica EM UC7. Thick (0.5–1 μm) sections were stained with the modified Methylene blue stain (Sokolova and Fuxa, 2008), examined and photographed under a Zeiss Axioplan microscope equipped with an Olympus DP73 digital camera. Thin (70–80 nm) sections were stained with uranyl acetate and lead citrate, and examined in a JEOL JEM 1011 microscope with the attached HAMAMATSU ORCA-HR digital camera. All reagents for LM were from Sigma–Aldrich (St. Louis, MO, USA), and for EM from EMS Chemicals (Fort Washington, PA, USA).

2.3. Spore purification and DNA isolation

Spores were extracted from heavily infected tissues previously stored at −20 °C. Briefly, thawed tissues were homogenised using a Teflon pestle in a 15 ml Wheaton tissue grinder, resuspended in PBS and filtered through cheesecloth to remove larger debris. The resulting spore suspension was then washed 2–3 times in 15 ml tubes with PBS by 10 min centrifugation at 3,000*g* (AccuSpin Centrifuge, Fisher Scientific, USA). The final pellet was resuspended in 5 ml of PBS, placed on 100% Percoll (Sigma–Aldrich) in 15 ml tubes and centrifuged at 600*g* for 35 min. Following centrifugation, cleaned spores were resuspended in PBS and their purity and integrity was inspected under a phase contrast microscope using 10–15 μl aliquots of spore suspension. Finally, spores were transferred to 1.5 ml tubes, washed three additional times in PBS by centrifugation (3,000*g*; Eppendorf centrifuge 5415C), and the final pellet was resuspended in 150 ml of TAE buffer (0.04 M Tris acetate, 0.01 M EDTA).

To release the DNA content from the spores, 150 mg of 0.1 mm glass beads were added to each tube and shaken with a BulletBlender™24 bead-beater (Next Advance, Inc., Averill Park, NY, USA) for 1 min at the maximum speed. The tube was then immediately placed onto a hot plate at 95 °C for 3–5 min, after which it was placed on ice. Suspension was checked again under the phase contrast optics for ruptured spores and used directly or diluted 10 or 100 times as a DNA template for PCR amplification (Vossbrinck et al., 2004).

2.4. PCR and sequencing procedures, and draft genome assembly as a source of tubulin sequences

The ssrRNA sequence from the Louisiana isolate of *A. penaei* (*A. penaei*–LA) was amplified using a PCR procedure with 1–3 μl of ruptured spore suspension as a DNA template, the OneTaq® Quick-load® master mix (New England Biolabs, Inc., Ipswich, MA, USA), and the following primers: 18f (5′-CAC CAG GTT GAT TCT GCC TGA C-3′) and 1492r (5′-GGT TAC CTT GTT ACG ACT T-3′) (Vossbrinck et al., 2004). Each PCR cycle included an initial denaturation step at 95 °C for 5 min, followed by 35 cycles with a denaturation at 95 °C for 30 s, annealing at 45 °C for 60 s and elongation at 72° for 120 s, with a final extension at 72 °C for 10 min. Amplicons were loaded onto a 2% agarose gel and bands of the expected size (1,200 bp) were excised and purified using a QIAquick Gel Extraction Kit (QIAGEN, Germantown, MD, USA). The purified PCR band was sequenced with the Applied BioSystems BigDye Terminator technology (version 3.1) and the resulting chromatogram was obtained using a Beckman Coulter Seq 8000 DNA. The primers for sequencing were V1, 530r (5′-CCG CGG C(T/G)G CTG GCA C-3′), 530f (5′-GTG CCA GC (G/A) GCC GCG G), 1061f (5′-GGT GGT GCA TGG CCG-3′), and 1492r (Vossbrinck et al., 2004). These primers produced overlapping sequences that were assembled with ChromasPro. 1.34 software (http://www.technelysium.com.au/ChromasPro.html). Direct PCR amplification and sequencing were performed at least twice for each DNA sample from a total of four samples from four shrimp, collected at different dates. Consensus sequence of the *A. penaei* small subunit was deposited in GenBank under accession number KF549987.

The amino acid sequences of the alpha- and beta-tubulins of *A. penaei*–LA were obtained from an ongoing genome sequencing project of this isolate and were deposited in GenBank under the accession number PRJNA206557. Preliminary genome assembly was obtained by subjecting DNA isolated from clean spores of *A. penaei* to Illumina MiSeq with 250 bp paired ends; a procedure that produced 12,855,013 pairs of reads. Paired-end reads were later assembled with MIRA v3.9.18 and the assembly was mined locally for genes encoding α- and β-tubulins using tBLASTX and tBLASTn (Altschul and Koonin, 1998). This search retrieved one single orthologue of each gene. The sequences were deposited in GenBank under accession numbers KJ579182 (alpha-tubulin) and KJ579183 (beta-tubulin).

2.5. Phylogenetic analysis

For the ssrRNA phylogeny, 50 sequences were retrieved from GenBank. The selected sequences included the closest matches in a BLAST search and other sequences of microsporidia that infect crustaceans and fish (Table 2). In addition, the sequences of microsporidia for which alpha- and beta-tubulin genes were available were added to the datasets for consistent comparison of topologies of the ssrRNA- and tubulin genes-inferred trees. One of the important goals we pursued in reconstructing ssrDNA-based phylogeny was to discover how the novel species is related to other

Table 2
Microsporidia from crustaceans and fish included in ssrDNA-inferred phylogenetic analyses.

Species	Host	Recorded Distribution	Env	Tissue tropism	GenBank accession number
Agmasoma penaei Louisiana (LA) isolate	*Litopenaeus setiferus* Decapoda, Peneidae	Atlantic, Gulf of Mexico	MB	Gonads	KF549987
Agmasoma penaei Thailand isolate	*Litopenaeus vannamei* Decapoda, Peneidae	Pacific, Thailand coast	MB	Muscles, hepatopancreas	DQ342240
Amezon michaelis	*Callinectes sapidus* Decapoda, Portunidae	Atlantic, Gulf of Mexico	MB	Hepatopancreas, hemocytes, muscles	L15741
Amezon pulvis	*Carcinus maenas*, Decapoda, Portunidae	Atlantic, Great Britain (GB) coast	M	Muscles	KC465966
Anostracospora rigaudi	*Artemia* spp. Anostraca, Artemidae	France, Ukraine	S	Intestine	JX915758
Areospora rohanae	*Lithodes santolla* Decapoda, Lithodidae	Pacific, Argentina	M	Phagocytes, connective tissue	Dr. Stentiford in person
Desmozoon lepeophtherii	*Lepeophtheirus salmonis* Copepoda, Caligidae	Worldwide	M	Hypodermis, connective tissues	HM800847
Enterocytospora artemiae	*Artemia* spp. Anostraca, Artemidae	United States of America (USA), France, Israel	S	Intestine	JX915760
Enterocytozoon hepatopenaei	*Penaeus monodon* Decapoda, Peneidae	Pacific	M	Hepatopancreas, intestine	FJ496356
Enterospora canceri	*Cancer pagarus* Decapoda, Canceridae	Atlantic, GB coast	M	Hepatopancreas, intestine	HE584634
Fascilispora margolisi	*Leoeophtherius salmonis* Copepoda, Caligidae	Pacific, British Columbia	M	Hypodermis, connective tissues	HM800849
Glugea anomala	*Danio rerio*, Actinopterygii, Cyprinidae	Worldwide	F	Various tissues, hypodermis, gut	AF044391
Hamiltosporidium magnivora	*Dapnia magna* Cladocera, Daphniidae	Russia	F	Fat body, hypodermis, ovaries	AJ302318
Hamiltosporidium tvaerminnensis	*Dapnia magna* Cladocera, Daphniidae	Northern Europe	F	Fat body, hypodermis, ovaries	GQ843833
Hepatospora eriocheir	*Eriocheir sinensis* Decapoda, Varumidae	Thames estuary, United Kingdom	F B	Hepatopancreas	HE584635
Heterosporis anguillarum	*Anguilla japonica* Actinopterygii, Anguilidae	East China Sea	F M	Muscles	AF387331
Larssonia obtusa	*Dapnia magna* Cladocera, Daphniidae	Northern Europe	F	Fat body, hypo-dermis, ovaries	AF394527
Microsporidium sp. 3	*Artemia franciscana* Anostraca, Artemidae	USA	S	No data	JX839890
Microsporidium sp. daphnia	*Dapnia pulex*, Cladocera, Daphniidae	Worldwide	F	Fat body	AF394528
Microsporidium sp. metapenaeus	*Metapenaeus joineri* Decapoda, Peneidae	Pacific, Japan coast	M	Muscles	AJ295328
Mrazekia macrocyclopis	*Macrocyclops albidus* Copepoda, Cyclopidae	Europe	F	Fat body	FJ914315
Myospora metanephrops	*Metanephros challenger* Decapoda, Nephropidae	South Pacific, New Zealand	M	Muscles	HM140497
Nadelspora canceri	*Metacarcinus magister* Decapoda, Canceridae	Atlantic	M	Muscles	AY958070
Nucleospora salmonis	*Oncorhynchus tshawytscha* Actinopterygii, Salmonidae	Atlantic	MF	Kidney	U78176
Perezia nelsoni[a]	*Litopenaeus setiferus* Decapoda, Peneidae	Atlantic, Gulf of Mexico	MB	Muscles	AJ252959
Spraguea lophii	*Lophius* spp. Actinopterygii, Lophiidae	Worldwide	M	Nervous system	AF033197
Thelohania butleri	*Pandalus jordani*, Decapoda, Caridea	Pacific, Canada, coast	M	Muscles	DQ417114
Thelohania contejeani	*Austropotamobius pallipes*, *Pacifastacus leniusculus* Decapoda, Astacidae	Europe	F	Muscles	AM261747
Thelohania montirivulorum	*Cherax destructor* Decapoda, Parastacidae	Australia	F	Muscles	AY183664
Triwangia caridinae[b]	*Caridina formosae* Decapoda, Caridiidae	Taiwan	F	Hepatopancreas, intestine, gills	JQ268567
Tuzetia weidneri[c]	*Penaeus aztecus* Decapoda, Peneidae	Atlantic, Gulf of Mexico	MB	Muscles	AJ252958
Outgroup: *Paranosema grylli*	*Gryllus bimaculatus* Orthoptera, Gryllidae	Eurasia	T	Fat body	AY305325

Env, Environment; M, marine; F, fresh water; B, brackish waters; S, salt lakes; T, terrestrial.
[a] *Pleistophora* sp. LS in GenBank.
[b] *Microsporidia* sp. CHW-2012 in GenBank.
[c] *Pleistophora* sp. (PA) in GenBank.

microsporidia parasitising decapods, including the Thailand isolate of *A. penaei* (*A. penaei*–Thai). To address this issue and given that eight of 15 ssrDNA sequences of decapod microsporidia available in GenBank covered only 720–900 bp of the query sequence (the one of *A. penaei*–LA), the first alignment we created contained 27 sequences, each 720 bp long, trimmed at the 5′ end at the position

395 to match the shortest sequence in the set, that of *A. penaei*–Thai (DQ342240). The sequence of *Enterospora canceri* (HE584634) was excluded from the final analysis because it overlapped with the aligned region of the gene by only 279 bp. The second dataset contained 42 1232 bp long sequences corresponding to the length of the shortest in this series *Mrazekia macrocyclopis* sequence (FJ914315). The sequences of both sets were aligned with Muscle (MEGA 5.05), with default parameters (Edgar, 2004). The first and second datasets resulted in 559 and 941 informative positions, respectively. Pairwise genetic distances were calculated by the Kimura-2 parameter method with a gamma distribution of 1 (Tamura et al., 2011). The alignments were subjected to phylogenetic reconstructions by maximum likelihood (ML) (MEGA 5.05, (Tamura et al., 2011) and Bayesian algorithms (MrBayes 3.2, (Ronquist et al., 2012)). ML phylogenetic analyses were conducted by PHYML using a GTR-γ model of nucleotide substitution (Nei and Kumar, 2000) as suggested by Modeltest, with1000 bootstrap replications. Bayesian inference was performed using the GTR model with five discrete gamma substitution categories, as well as a proportion of invariable sites. Analysis was performed with a sampling frequency of 250 with four parallel chains and default priors. *Paranosema grylli* (Microsporidia) and *Rozella allomycis* (Cryptomycota (James et al., 2013 or Rozellomicota (Corsaro et al., 2014)) were used as outgroups for phylogenetic reconstructions using, respectively, the first and second datasets.

Agmasoma penaei tubulin gene sequences were retrieved from a draft genome assembly of this species and used for phylogenetic reconstruction using 24 available sequences from other microsporidian species and from *R. allomycis*. Retrieved sequences were aligned using MUSCLE (Edgar, 2004), and concatenated to produce a supermatrix of 777 amino acids in length. ML analysis was performed using PHYML with the LG + G + I model as suggested by ProtTest (Darriba et al., 2011) with 1,000 bootstraps replicates. In parallel, Bayesian analyses were performed using PhyloBayes

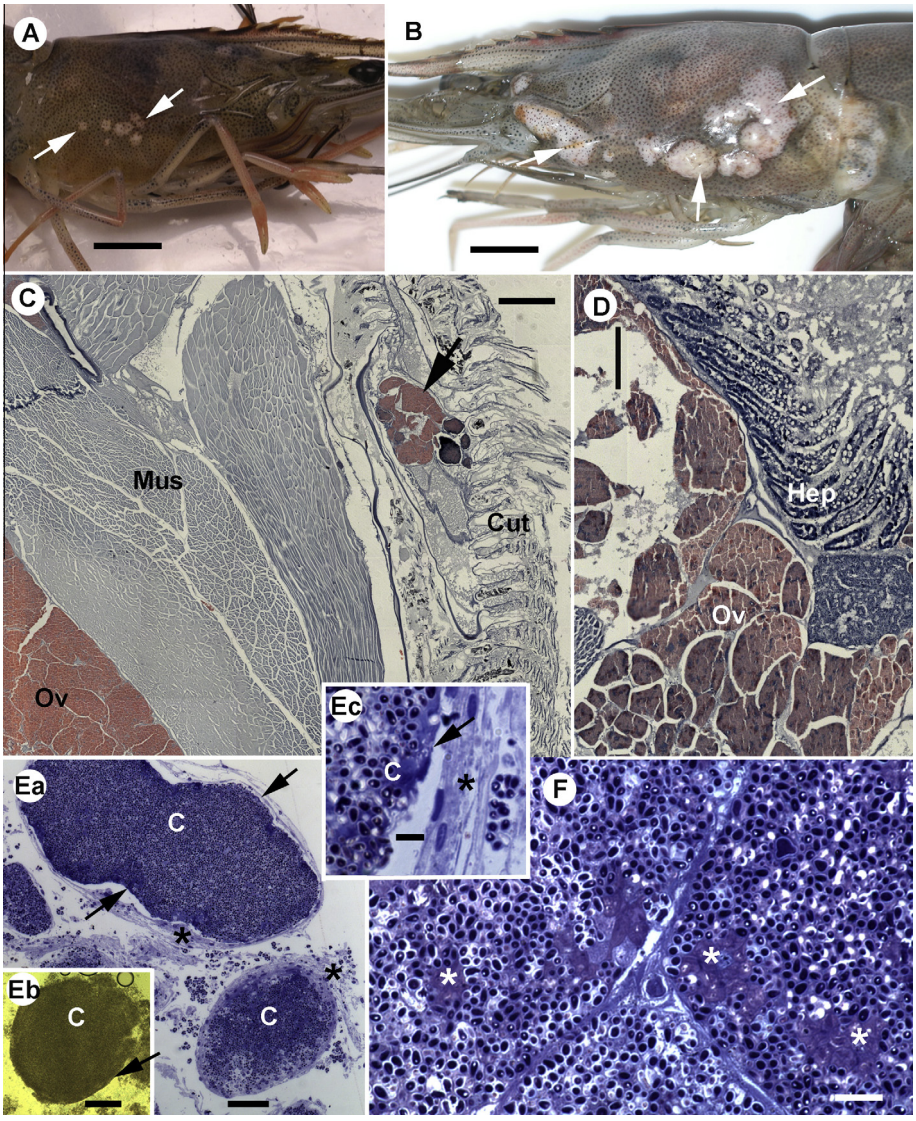

Fig. 1. Gross pathology and tissue tropism for *Agmasoma penaei*. (A) Subcuticular cyst-like or small tumour-like masses (arrows) visible through transparent chitinous cuticle; scale bar = 1 cm. (B) Hypertrophied masses of microsporidium-infected ovarian tissue inside the carapace; scale bar = 1 cm. (C, D) Paraffin sections through carapace stained with Luna stain. Tissues infected with microsporidia, ovaries (Ov) and subcuticular spore masses (arrow) are stained pink (dark grey). Muscles (Mus) and hepatopancreas (Hep) are not infected. C, scale bar = 500 μm; D, scale bar = 250 μm. (Ea) Thick section through cysts enclosed in thin envelopes (arrow) and covered with several layers of flattened haemocytes (asterisk); scale bar = 50 μm. (Eb) A cyst liberated from infected shrimp, live preparation; scale bar = 100 μm. (Ec) Thick section through the periphery of the cyst at larger magnification; scale bar = 5 μm. (F) Thick section through the ovary. Original tissue is completely replaced by microsporidian spores and pre-spore stages (asterisks); scale bar = 10 μm. (C–F) Bright field microscopy.

(Lartillot et al., 2009) (http://www.phylo.org/tools/pb_mpiManual1.4.pdf), with the CAT equilibrium frequency profile, the LG model and four discrete gamma categories, with two chains running until the maxdiff parameter dropped below 0.1, which is indicative of a good run.

3. Results

3.1. Gross pathology, tissue tropism and light microscopy

The external clinical signs of infection were as follows: (i) cyst-like or small tumour-like masses located beneath the chitinous cuticle of the carapace (Fig. 1A); (ii) shapeless masses of tissues located centrally inside the carapace (Fig. 1B); (iii) a narrow elongated formation in the shape of a cord extending dorsally along the abdomen from the carapace to the last segment (not shown). All of these formations were white, contrasted well against surrounding tissues and were clearly visible though the translucent cuticle. Microscopic examination of the white masses revealed mature spores that completely displaced the host tissue and obscured the nature of the type of parasitised tissue. Examination of paraffin Luna-stained sections and Epon–Araldite-embedded Methylene blue-stained sections proved that the infection was limited mainly to hypertrophied gonads (Fig. 1C, D, F). The dorsal cord was in fact the abdominal lobe of the ovaries. Sub-cuticular "cysts" and small tumour-like formations (Fig. 1A, B, Ea–c) were readily liberated from infection sites (Fig. 1Eb). The tumour-like growths measured 100–500 μm and were filled with numerous octets of mature spores enclosed in

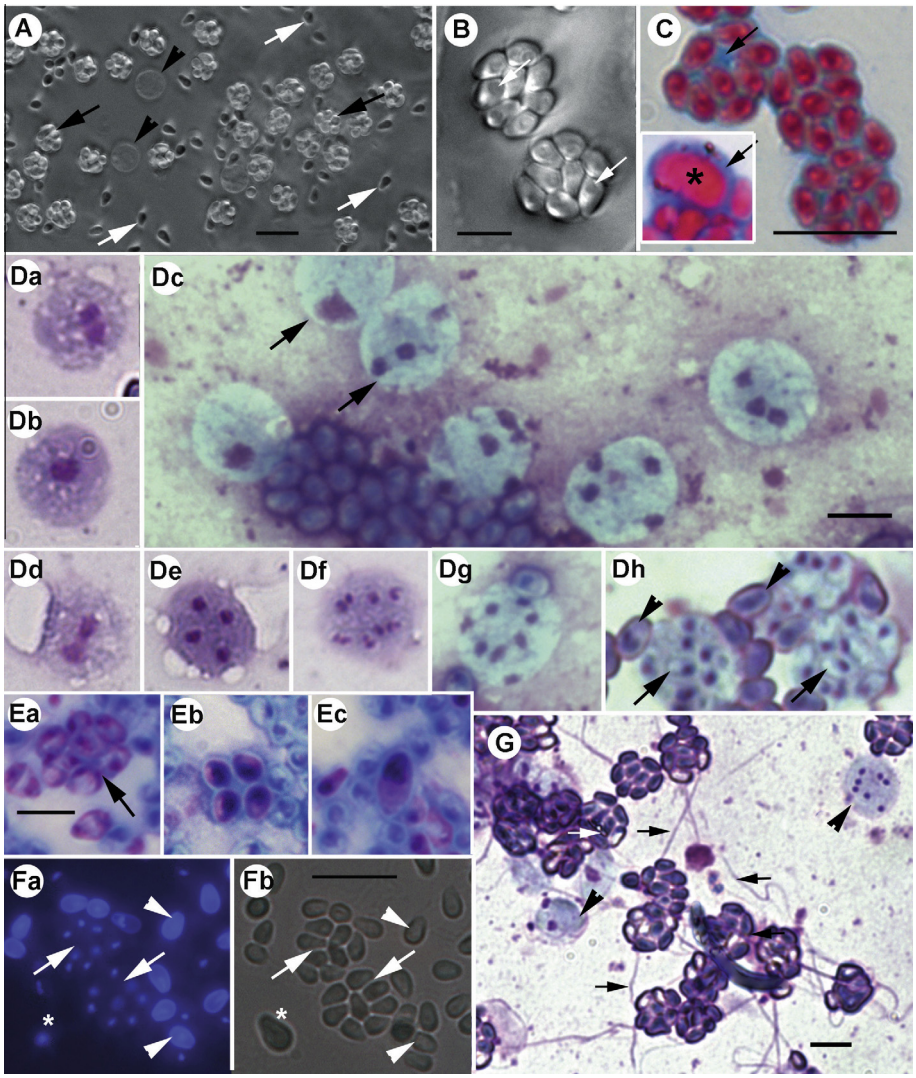

Fig. 2. Light microscopy of *Agmasoma penaei* showing spores and stages on smears. (A) Fresh smears from infected tissues under dark field optics. Octets of spores (black arrows), free spores liberated from sporophorous vesicles (SVs) (white arrows), and round sporonts (black arrowhead). (B) Two SVs at higher magnification, each containing eight pyriform spores. A round depression inside a spore (white arrow) corresponds to the posterior vacuole. (C) SVs and a macrospore (asterisk) on a methanol-fixed and Trichrome-stained smear; chitin component of spore walls is stained red, SV internal matrix is stained blue. (Da–h, Ea–c) Stages of the microsporidium lifecycle on methanol-fixed smears stained with Giemsa. (Da) A stage with paired nuclei; (Db) a stage with a single nucleus, presumably the product of merging of diplokaryon counterparts; (Dc) spores and sporonts with one to five nuclei; arrow points to stages with a dividing nucleus. (Dd) A stage with the nucleus in the process of division; (De) four-nucleate sporont; (Df,g) eight-nucleate sporonts splitting into eight sporoblasts; (Dh) immature SVs with sporoblasts (arrows), surrounded by more intensively stained mature spores (arrowheads). (Ea) Arrow points to SV with eight mature spores; (Eb) SV with four teratogenous macrospores; (Ec) SV with only one teratogenous macrospore. (Fa,b) A smear double-stained with Calcofluor and DAPI (a, fluorescent microscopy; b, bright field). Calcofluor exclusively stains mature spores with formed chitinous wall (arrowheads). SVs with immature spores are indicated by arrows. An immature macrospore is marked with an asterisk. (G) Giemsa-stained smear showing bi- and multi-nucleate sporonts (arrowheads) and sporophorous vesicles with mature spores. Extruded polar tubes are arrowed. Aa–h, C, Fa,b, G, scale bar = 1 μm; B, Da–h, Ea–c, scale bar = 5 μm. (For interpretation of the references to colour in this figure legend, the reader is referred to the web version of this article.)

thin, fragile, easily disrupted envelopes. Cysts were covered with several layers of flattened haemocytes (Fig. 1Ec). Muscle, gut epithelium and hepatopancreas were free of parasites, as suggested by examination of paraffin-embedded Luna stained sections (Fig. 1C, D).

Examination of fresh smears from infected tissues by dark field and phase contrast microscopy revealed numerous spores. Some spores were enclosed in SVs in sets of eight (Fig. 2A, B), while others were released from fragile SVs as individual spores. Live SVs measured 8.7 ± 0.10 × 7.1 ± 0.11 μm (n = 70), and ranged from 7.0–10.49 × 5.5–9.40 μm. Methanol-fixed and Trichrome- (Fig. 2C) or Giemsa-stained (Fig. 2D) SVs measured 8.7 ± 0.14 × 7.1 ± 0.11 μm (n = 40), and ranged from 7.1–10.8 × 5.6–8.8 μm. The membranes of mature SVs were easily disrupted upon spore maturation and/or physical pressure. For example, even delicate homogenisation of the infected tissue in a grinder caused splitting of octets into individual spores. Live spores were 3.5 ± 0.00 × 2.0 ± 0.02 μm (n = 102), ranging from 2.7–4.2 × 1.5–2.7 μm; methanol-fixed were – 3.3 ± 0.04 × 2.0 ± 0.03 μm (n = 78), ranging from 2.7–4.5 × 1.4–2.8 μm. In addition to SVs and free spores, roundish pre-spore stages of approximately the same sizes as SVs (Fig. 2A), and macrospores (5.8 ± 0.16 × 2.8 ± 0.01 μm (n = 10), ranging from 4.7–7.00 × 2.5–3.13 μm) were occasionally observed. Spores in methanol-fixed smears stained red with Trichrome. The internal matrices of immature SVs on Trichrome-stained smears were intensively stained with a counterstain Evans Blue, suggesting the presence of an organic matrix inside each vesicle (Fig. 2C). Staining with Giemsa revealed the following stages: stages with paired nuclei (Fig. 2Da), stages with a single nucleus (Fig. 2Db, Dc), and cells with two to eight nuclei, some in the process of division (Fig. 2Dc–Dg). Sporonts split into individual sporoblasts at the eight-nucleate stage within the pansporoblast membrane (which upon spore maturation became a SV membrane) (Fig. 2Dg, Dh). Normally each SV contained eight spores (Fig. 2Ea), but SVs with four, two or one "macrospores" were not uncommon (Fig. 2Eb, Ec) probably due to teratogenic sporogony. Spores, especially those liberated from subcuticular cysts, readily fired on smears (Fig. 2G). The length of a polar tube was approximately 40 μm. Staining with Calcofluor allowed us to distinguish between mature and immature spores: the future chitinous wall of immature spores was not completely formed and did not bind Calcofluor stain, while spore walls of mature spores exhibited bright fluorescence (Fig. 2Fa,b). Spores within SVs contained a single round or slightly elongated nucleus, clearly visible on DAPI- or Giemsa-stained smears (Fig. 2Ea, Fa,b).

3.2. Scanning electron microscopy (SEM)

Masses of SVs were visible in SEM samples of infected tissues. SVs appeared as sacs with eight spores inside or as "elastic" SV envelopes tightly enclosing spores (Fig. 3). Some SVs were broken and split in half, exhibiting an internal carcass which isolated spores from each other (Fig. 3A). Spores liberated from SVs were pyriform with relatively smooth surfaces (Fig. 3B). Fine tubules derived from the surface of some SVs and occasionally the tubules were associated with accumulation of filamentous material (Fig. 3C).

3.3. Transmission electron microscopy (TEM)

The earliest stages observed in TEM were diplokaryotic meronts (Fig. 4A). Meronts divided by binary fission; cells with two diplokaryons and diplokaryons in the process of division were not uncommon (Fig. 4Ba). Diplokaryotic meronts were often seen in chains, their nuclei exhibiting tight contact between two nucleus counterparts. Numerous vesicles and vacuoles, some of which derived from the enlarged regions of perinuclear space, were scattered over their cytoplasm (Fig. 4A, Ba). A meront was surrounded by a single electron-dense membrane of approximately 16 (13–19) nm thick. The integrity of the envelope was occasionally interrupted by electron-dense structures resembling pores, associated with tubular-like structures presumably excreted by meronts

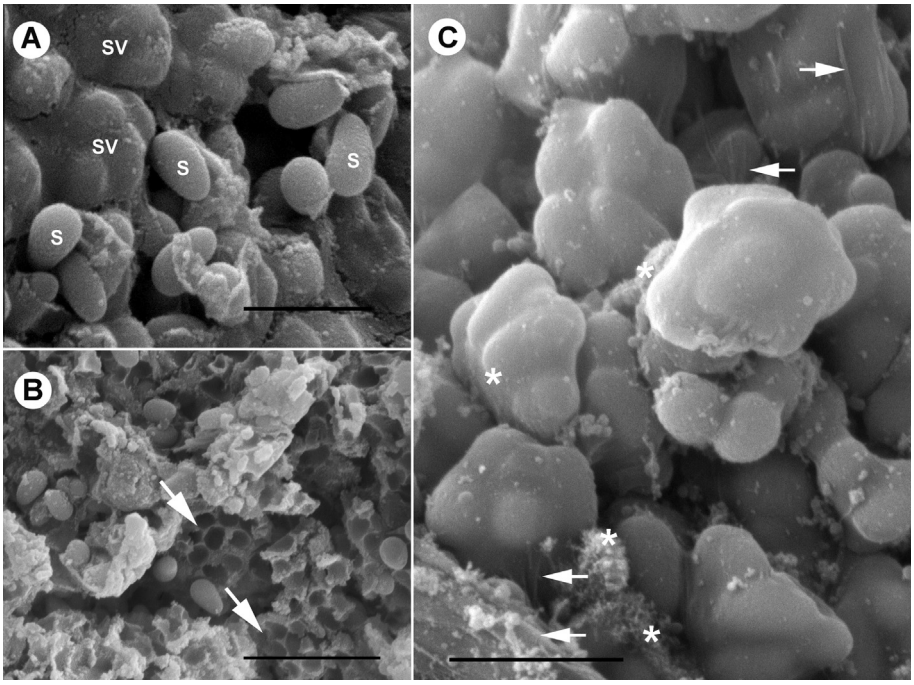

Fig. 3. Scanning electron microscopy of *Agmasoma penaei*. (A) Infected tissue is seen as a mass of sporophorous vesicles (SV) and free spores (S) released from SVs. (B) Some SVs are broken and exhibit an internal carcass, which isolates spores from each other within a SV (arrows). (C) "Elastic" SV envelopes tightly enclose the spores inside. Fine tubules originate from the surface of some SVs (arrows). Accumulation of filamentous material on the surface of SVs is indicated by asterisks. A, C, scale bar = 5 μm; B, scale bar = 10 μm.

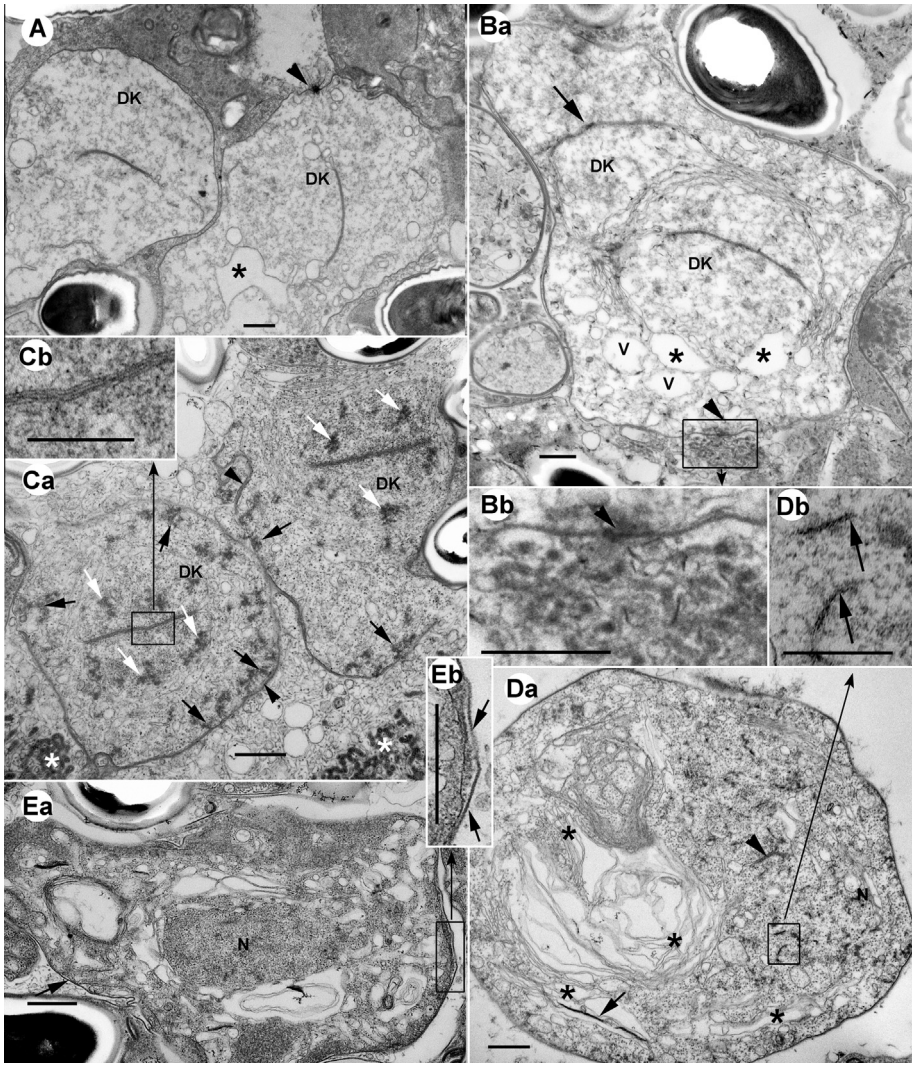

Fig. 4. Transmission electron microscopy of *Agmasoma penaei* showing merogony. (A, Ba,b) Early diplokaryotic meronts. (A) After completing cytokinesis, cells with diplokarya (DK) are staying together. Arrow points to a spindle plaque. Enlarged regions of perinuclear space are indicated by the asterisk. (Ba,b) Meront with two not yet dissociated diplokaria. V, vacuoles derived from the perinuclear space. Tubular-like structures are released into host cytoplasm through electron-dense structures resembling pores (boxed, enlarged on Bb, arrowhead). (Ca,b) Late diplokaryotic meronts with denser cytoplasm and characteristic electron-dense structures scattered through nucleoplasm (white arrows) and cytoplasm (black arrows). Asterisks indicate tubular material secreted at the earlier stage, and arrowheads the thickened cell envelope. All four membranes can be distinguished in the zone of contact of DK counterparts (boxed, enlarged in Cb). (Da,b). The meront-sporont transitional stage is undergoing meiosis marked by synaptonemal complexes in the nucleoplasm (boxed, enlarged on Db). The zone of contact between nuclei of the former diplokaryon (arrowhead) can hardly be seen. Numerous membrane profiles (asterisks) appear in the cytoplasm. Some of those contain strips of electron-dense material (arrow). (Ea,b) An additional membrane, corresponding to the wall of a future sporophorous vesicle, appears outside the sporont envelope at the transitional meront-sporont stage (boxed, enlarged in Eb, arrows). N, nucleus with synaptonemal complexes. A, Ba, Bb, Ca, Da, Ea, Eb, scale bar = 500 nm; Cb, Db, scale bar = 250 nm.

in the surrounding host cytoplasm (Fig. 4Ba,b). After a series of divisions, dikaryotic cells underwent transformation; their cytoplasm became denser and electron-dense structures appeared in the nuclei and surrounding cytoplasm. These structures often accumulated at the cell periphery in the vicinity of the cell membrane (Fig. 4Ca). The contact between nucleus counterparts became looser and four distinct membranes could be distinguished in the zone of contact (Fig. 4Ca, Cb). These changes indicated approaching karyogamy and meiosis. At the next stage of the life cycle, which can be designated as a sporont (or the mother cell of sporoblasts), synaptonemal complexes became visible in the nucleoplasm, indicating initiation of meiosis (Fig. 4Da, Db). The contact between diplokaryon counterparts was barely detectable (Fig. 4Da). The most characteristic feature of this stage was an abundance of membrane profiles, cisternae, vacuoles and membrane whorls inside the cytoplasm. Some cisternae contained strips of electron-dense material (Fig. 4Da). While sporont mother cells were undergoing meiosis, an additional layer split off the sporont envelope extracellularly, corresponding to the envelope of a future SV (Fig. 4Ea, Eb). The space between two envelopes (episporontal space) ultimately expanded and was filled with homogenous secreted material composed of fine granules (Fig. 5Aa, B). The electron-transparent cells surrounded by halos of dense secretions, deposited inside episporontal spaces (Fig. 5Aa), were the second most abundant stage in sections through infected tissues, after SVs with mature spores. The clumps of tubular material resulting from meront secretion (Fig. 4Bb) were consistently observed adjacent to SV envelopes (Fig. 5Aa). Sporont envelopes looked uneven due to deposits of electron-dense material (Fig. 5Aa,b). Each sporont contained a large centrally located nucleus. The presence of spindle plaques and kinetochore-like structures (Fig. 5Aa,c) suggested some cells were in the process of nuclear division. At the next stage, referred to as a multinucleate sporont, at least two peripherally-located nuclei could be observed inside the parasite cells (Fig. 5B). The

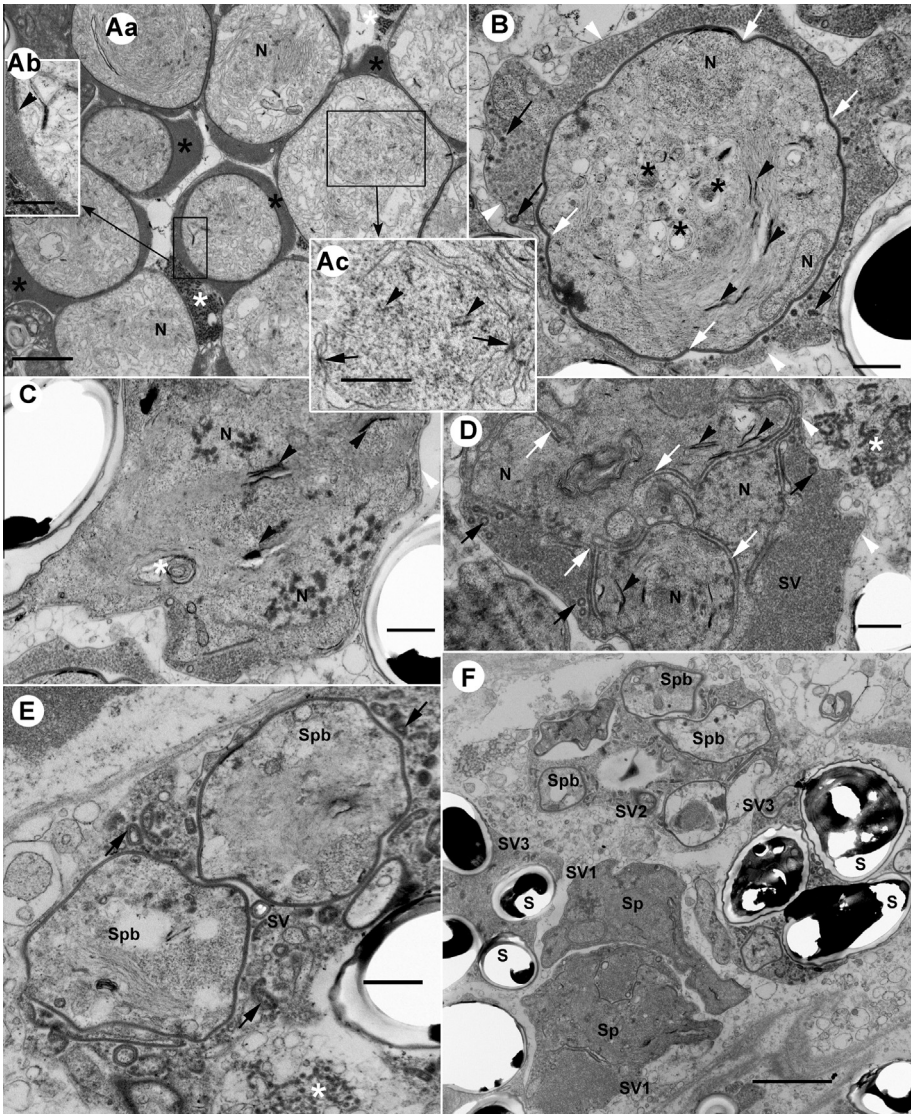

Fig. 5. Transmission electron microscopy of *Agmasoma penaei* showing sporogony. (Aa–c) Section through sporonts residing in sporophorous vesicles (SV) filled with dense homogenous material (black asterisks). Sporont membrane is thickened with deposits of electron-dense material (boxed, enlarged in Ab, arrowhead). Clumps of tubular material in the host cytoplasm adjacent to SV envelopes are indicated by white asterisks. Each sporont contains a large, centrally located nucleus (N). Portion of nucleus with spindle plaques (arrows) and kinetochore-like structures (arrowheads) is boxed and enlarged in Ac. The presence of these structures suggest the cell is undergoing nuclear division. (B, C) Multinucleate sporonts with at least two peripherally-located nuclei (N) in the view. Continuous electron-dense envelope of the sporont exhibits curvatures (B, white arrows). SVs are limited by thin membrane (white arrowheads). Inclusions of higher electron density (black arrows) appear among fine granular material filling SV lumen. Strips of electron-dense material are deposited inside membrane cisternae (black arrowheads). Roundish vacuoles with electron dense cores (B, black asterisks) and whorls of membranes (C, white asterisk) are typical cell components at this stage. (D) Multinucleate sporont in the process of splitting into sporoblasts: nuclei with adjacent cytoplasm are becoming segregated by invaginations of the sporont envelope (white arrows) and strips of electron-dense material (black arrowheads). White arrowheads indicate SV membrane; a white asterisk shows a conglomerate of tubular secretion material, still abundant in host cells in the vicinity of parasites. (E) SV containing two sporoblasts (Spb) is filled with contours of material (arrows) similar in consistency and thickness to the envelope of the mother sporont cell. (F) Section through infected tissue demonstrates SVs enclosing parasites at different stages of sporogony: SV1, multinucleate sporonts (Sp); SV2, sporoblats (Spb); SV3, spores (S). Aa, F, scale bar = 2 μm; Ab, Ac, scale bar = 1 μm; B–F, scale bar = 500 nm.

envelopes around sporonts became continuous and thicker (39–47 μm thick). Simultaneously, electron-dense inclusions appeared within SV lumens (Fig. 5B). In the cell cytoplasm, the strips of electron-dense material deposited inside membrane cisternae became more numerous. Roundish vacuoles with an electron-dense core and whorls of membranes were typical components of sporonts at this stage (Fig. 5B). Multinucleate sporonts eventually split into eight sporoblasts (Fig. 5E, F), and transitional cells of irregular shape were occasionally seen in sections through infected ovaries (Fig. 5C, D, F). Nuclei with adjacent cytoplasm were isolated from each other by the cisternae with strips of electron-dense material and invaginations of the sporont envelope. SVs containing sporoblasts were filled with material similar in consistency and thickness to the sporoblast walls (Fig. 5E). Sporoblasts were uninucleate and demonstrated vacuolated cytoplasm with numerous membrane cisternae and vesicles, among which a large container, presumably with the precursor of the anchoring disk, could be distinguished. Sporoblasts were enclosed in 35–45 nm thick envelopes (Fig. 6A, B). Mature spores resided in SVs, each limited by a thin membrane. The tubular electron-dense secretion was not observed in SVs with mature spores (Fig. 6D).

Spores (Fig. 6D) on thin sections averaged 2.4 × 1.2 μm (2.1–2.6 × 1.0–1.4). Macrospores were approximately twice that size (3.6 × 2.5 μm). Their atypical internal structure, including several nuclei and chaotic distribution of polar filament coils (Fig. 6C), suggested those were teratogenic non-viable products of abnormal

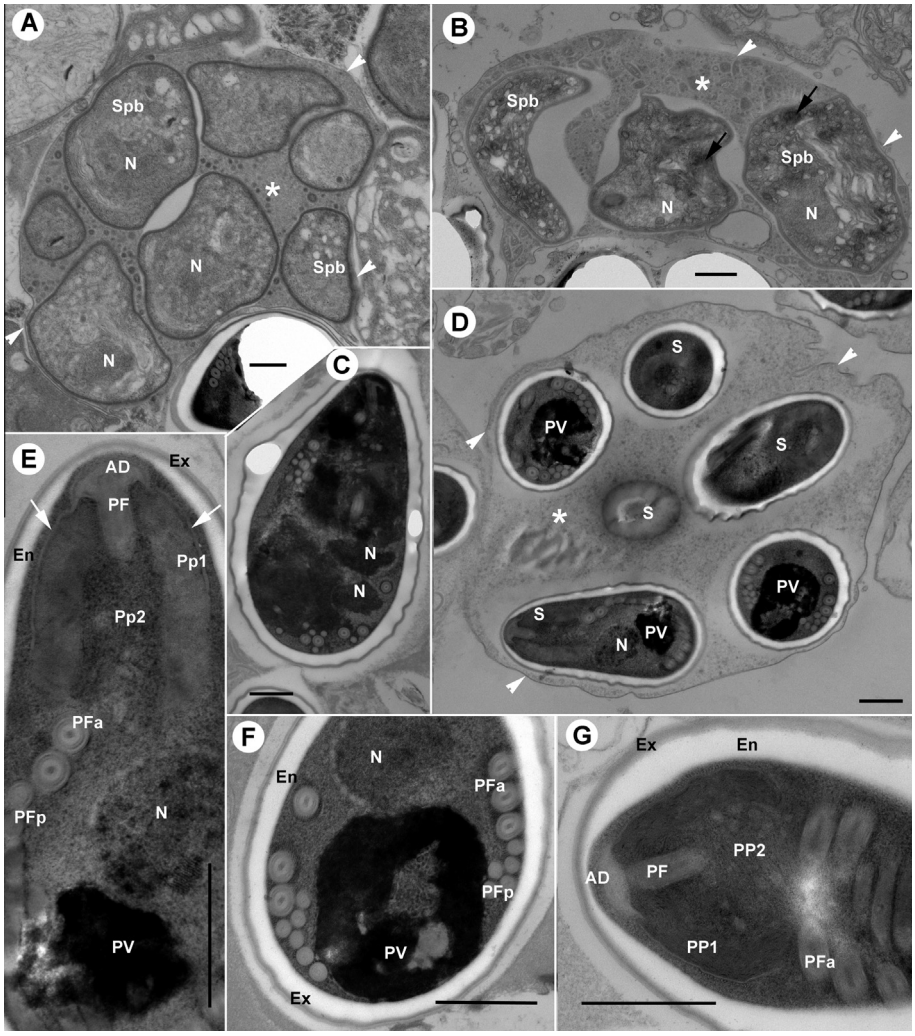

Fig. 6. Transmission electron microscopy of *Agmasoma penaei* showing sporoblasts and spores. (A, B) Sporophorous vesicles (SVs) with sporoblasts (Spb) are limited by a fine membrane (white arrowheads). SV lumen (asterisk) is filled with fine granular material and occasional electron-dense inclusions. N, sporont nucleus. Black arrows point to anchoring disk precursors. (C) A macrospore (teratospore) is approximately twice the size of a regular spore (compared with D). It contains several nuclei (N) and chaotically distributed polar filament coils. (D) SV with mature spore (arrowheads point to the SV membrane). SV lumen (asterisk) does not contain electron-dense inclusions. N, spore nucleus; PV, posterior vacuole; S, spores. (E–G) Details of the spore ultrastructure. AD, anchoring disc; En, endospore; Ex, exospore; N, nucleus; PF, polar filament; PFa, anterior polar filament coils; PFp, posterior polar filament coils; Pp1, lamellar polaroplast; Pp2, vesicular polaroplast; PV, posterior vacuole. Arrows point to the polar sac. A–G, scale bar = 500 nm.

sporogony. Regular spores had an electron-translucent endospore that was 100–120 nm thick (except for the anterior end), and a three-layered exospore which was approximately 30–50 nm thick. Polar filaments were anisofilar, with two or three anterior coils of larger diameter (141 nm in average, range 122–166 nm) and from four to six posterior coils (87 nm in average, range 59–101 nm). Larger coils demonstrated a multilayered structure in cross sections (Fig. 6E–G). The prominent posterior vacuole was up to 949 nm in diameter (725 nm on average) and was limited by a membrane. The internal structure was poorly preserved (Fig. 6D–F), but remains of tubular secretion were visible in some sections (Fig. 6F), suggesting it was in fact a posterosome. A single nucleus was centrally located and measured 516–703 nm in diameter (595 nm on average) (Fig. 6D, E). The polaroplast was composed of two parts: the external (lamellar) part of tightly packed membranes, and internal vesicular region built of vesicle-like loosely arranged membrane profiles (Fig. 6G). A mushroom-shaped polar disc formed a continuum with the anterior part of the polar filament (Fig. 6E). A polar sac embraced the external part of the polaroplast.

3.4. Phylogenetic relationship of A. penaei–LA with other microsporidia based on ssrRNA

The recovered 1271 nucleotide sequence of ssrDNA of *A. penaei*–LA shared significant similarities with many orthologues deposited in gene databases and particularly with a 720 bp long sequence from *A. penaei* Thai (DQ342240). The pairwise divergence value ("evolutionary distance") between two geographical isolates of *A. penaei* was 0.066, as suggested by pairwise distance analyses of the alignment of 27 × 720 nucleotide long sequences (Table 3). Alignment of ssrDNA sequences of Thailand and Louisiana *A. penaei* isolates revealed several mismatches, including a 4 bp repeat that appears to be specific to the Thailand isolate (Fig. 7). The genetic similarity of the *Agmasoma* isolates was closest to *Enterocytozoon hepatopenaei* (value of sequence divergence, 0.278) and *Hepatospora eriocheir* (0.282), the parasites of decapods, *M. macrocyclopis* (0.276) and *Desmozoon lepeophtherii* (0.284), microsporidia infecting free-living and parasitic copepods, respectively, *Microsporidium* sp. from cladocerans of the genus *Daphnia* (0.257) and *Nucleospora salmonis* (0.281) from fish. Other sequences in this alignment,

Table 3
Evolutionary distances between ssrDNA sequences of various taxa.

Microsporidia species	*Hamiltosporidium tvaerminnensis*	*Trachipleistophora hominis*	*Encephalitozoon hellem*	*Glugea anomala*	Louisiana isolate[a]	*Nosema apis*	*Desmozoon lepeophtherii*	*Ameson michaelis*
Hamiltosporidium magnivora	0.004							
Vavraia culicis		0.038						
Encephalitozoon romaleae			0.050					
Heterosporis anguillarum				0.055				
Thailand isolate[a]					**0.066**			
Nosema ceranae						0.069		
Nucleospora salmonis							0.078	
Ameson pulvis								0.095

Bold value indicates the difference between two geographical isolates of *Agmasoma penaei*.
[a] An isolate of *Agmasoma penaei*.

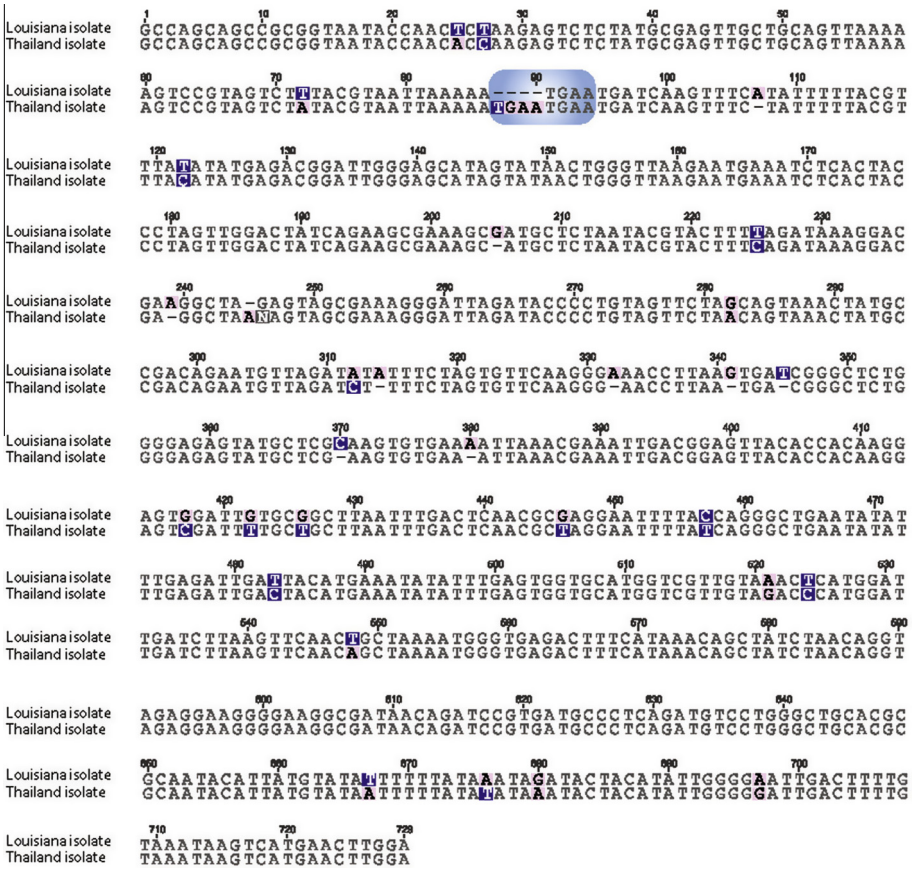

Fig. 7. Alignment of ssrDNA sequences from the Thailand and Louisiana isolates of *Agmasoma penaei*. A total of 694 identical sites out of the total 729 sites show a similarity of 95.2%, with base pairs in divergent sites highlighted in light pink (light grey) for purines and dark blue (dark grey) for pyrimidines. A short tandem repeat of 4 bp is surrounded by a rounded rectangle, being present twice in the Thailand isolate but only once in the Louisiana isolate. Black circles indicate bootstrap values and Bayesian posterior probabilities of 100%. (For interpretation of the references to colour in this figure legend, the reader is referred to the web version of this article.)

including those belonging to microsporidia from decapods and penaeid shrimps, exhibited only 0.383–0.535 of ssrDNA sequence divergence with the *A. penaei*–LA sequence. The most divergent sequence (0.535) in this series was the one of *Ameson michaelis*, the microsporidium infecting blue crabs, *Callinectes sapidus*, which shares habitat with *L. setiferus* in the Gulf of Mexico. On the phylogenetic tree (Fig. 8), most sequences of microsporidia from decapod crustaceans split among two major well-supported lineages. Only *Areospora rohanae* clustered with the *Hamiltosporidium* branch, although with extremely low support, leaving the position of this species unresolved. Most decapod taxa appeared to belong to the lineage which also included microsporidia infecting fish (*Sparguea lophii*, *Glugea anomala* and *Heterosporis anguillarum*), as well as *Facilispora margolisi*, a copepod hyperparasite of sea lice *Lepeophtherius salmonis* (Jones et al., 2012).

In our phylogenetic reconstructions, *A. penaei*-LA clustered together with A. *penaei*-Thai, within a lineage that included two microsporidia from decapods, *E. hepatopenaei* and *H. eriocheir*, as well as *Microsporidium* sp. from *Daphnia*, the dichotomy *D. lepeophtherii*–*N. salmonis*, and *M. macrocyclopis* from a free-living copepod *Macrocyclops albidus*. The latter taxa clustered with moderate but statistically confident support with the *A. penaei* branch. The *Thelohania* spp., *Hamiltosporidium* spp. and *Larssonia obtusa* branches formed separate lineages.

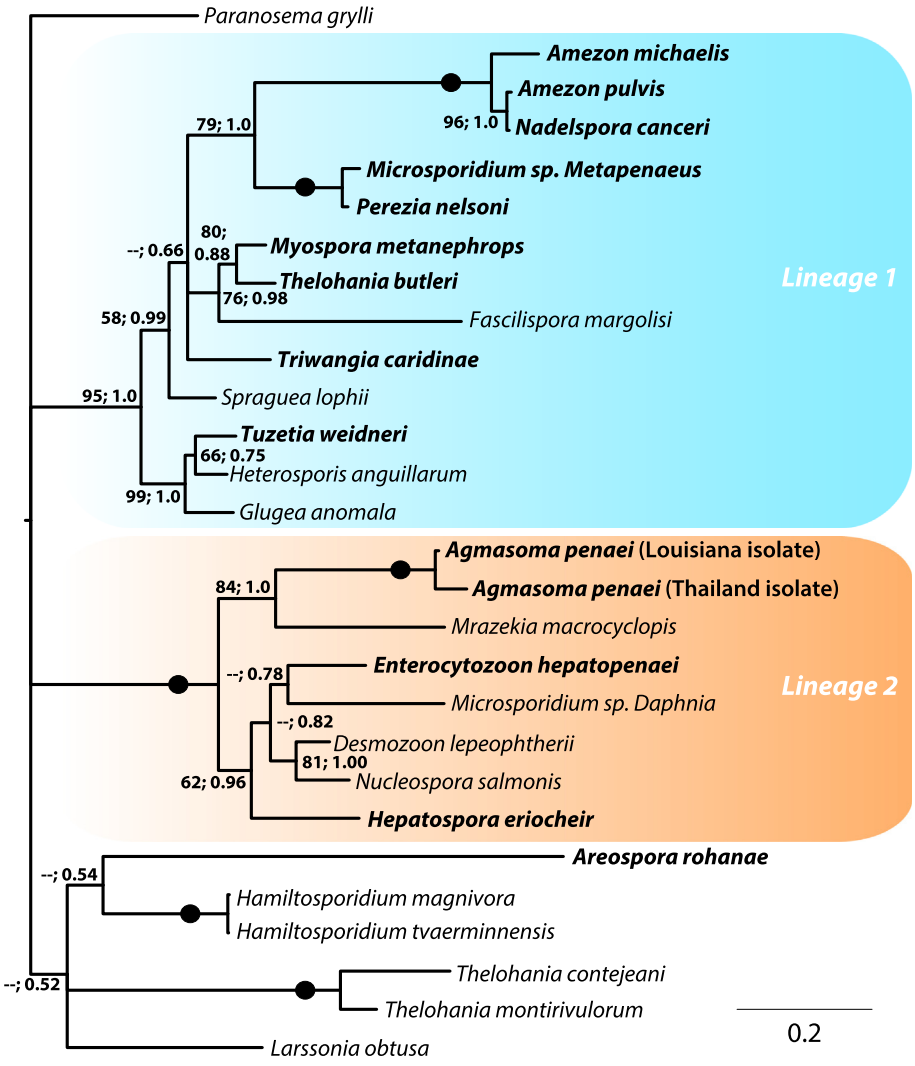

Fig. 8. ssrDNA-inferred Bayesian tree based on 559 informative positions of 27 × 720 bp long microsporidian sequences. Bootstrap values of maximum likelihood (ML) analysis are shown first, followed by posterior probabilities of Bayesian analysis (GTR + Γ4 models of evolution for both analyses). The branches with less than 50% nodal support in Bayesian analysis are shown as polytomies. Microsporidia infecting marine and brackish water decapods (bold) except *Areospora rohanae*, fell into two well-supported lineages (rounded rectangles). The *Agmasoma* branch clusters within Lineage 2. Black circles indicate ML bootstrap values and Bayesian posterior probabilities of 100%. Scale bar corresponds to 0.2 substitutions per site.

Bayesian and ML analyses applied to the second alignment of 42 × 1271 bp long sequences resulted in an identical tree topology (Fig. 9A). The increase in informative characters and the number of included taxa, as well as elimination of short sequences, did not affect branching of the remaining taxa (Figs. 8 and 9A), but better resolved the position of *A. penaei*–LA. Specifically, the latter appeared as a basal and significantly diverged taxon (Fig. 9A; Supplementary Table S1), falling within a dichotomy with a cluster of species containing crustacean microsporidia (*M. macrocyclopis* and two species from *Artemia*), as well as human microsporidium *Vittaforma corneae* and *Endoreticulatus* sp. from lepidopterans. The *Agmasoma–Mrazekia–Endoreticulatus* lineage was well supported and emerged as a sister group to the *Nucleospora–Enterocytozoon* clade (Fig. 9A).

Overall, the resulting tree identified several clades (Fig. 9A) with branching in good agreement with previously published ssrDNA-inferred phylogenies (Stentiford et al., 2010, 2013a,b; Jones et al., 2012; Rode et al., 2013). The two clades with highest support were the *Ameson–Trachipleistaphora–Glugea–Spragiea* clade and the *Nosema–Encephalitozoon–Enterocytozoon–Endoreticulatus–Agmasoma* clade. The former clade corresponded to the clade Marinosporidia (Clade II, microsporidia of saltwater origin sensu Vossbrinck, Debrunner-Vossbrinck, 2005), and contained all microsporidia from decapods presented in this analysis, except for *A. penaei*. The latter was congruent with the clade Terresporidia (Clade IV, microsporidia of terrestrial origin sensu Vossbrinck, Debrunner-Vossbrinck, 2005) and included *A. penaei*.

3.5. Phylogenetic relationship of *A. penaei*–LA with other microsporidia based on alpha- and beta-tubulin sequences

Phylogenetic reconstructions performed using a concatenation of α- and β-tubulin sequences resulted in well-supported nodes (Fig. 9B), with a branching that is in overall agreement with previous analyses based on the same genes (Lee et al., 2008; Corradi et al., 2009). The tubulin phylogeny strongly confirmed the placement of *A. penaei* within the Clade IV sensu Vossbrink, Debrunner-Vossbrinck (2005), and highlighted an extreme divergence of the *A. penaei* branch.

3.6. Taxonomic summary

In this study we provide the taxonomic description of the genus *Agmasoma* and its type species *A. penaei*,, updating that of Hazard and Oldacre (1975).

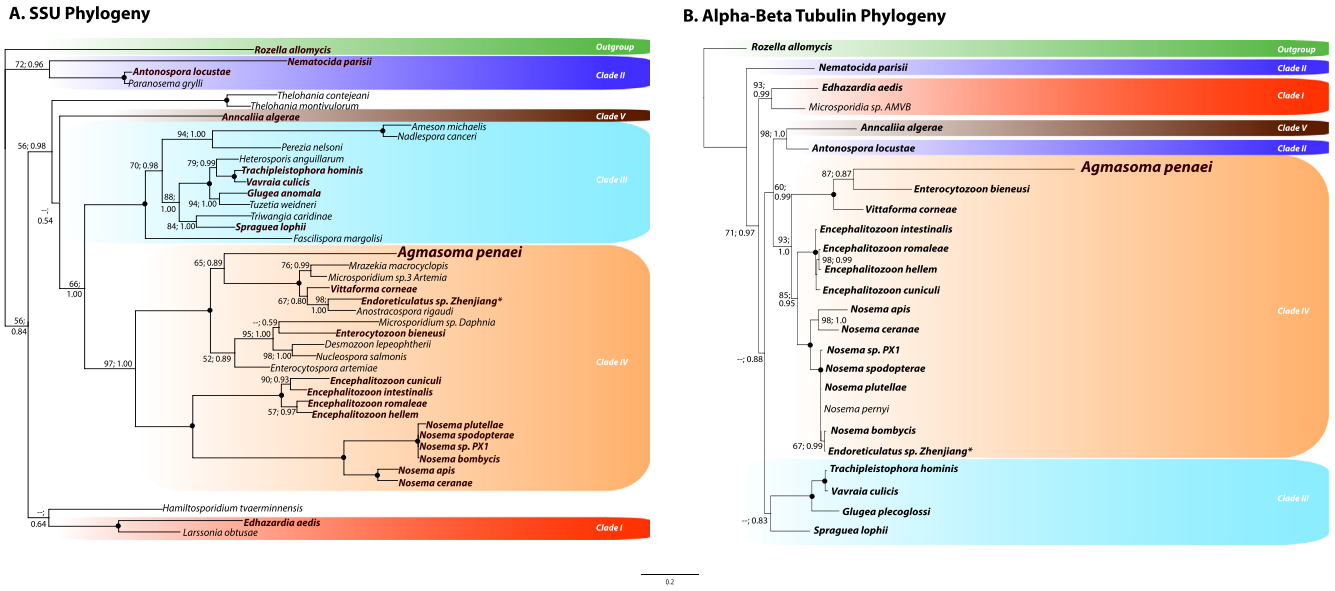

Fig. 9. Microsporidian phylogeny inferred from (A) ssrDNA and (B) the concatenation of the alpha- and beta-tubulin genes. Taxa belonging to major microsporidian clades (after Vossbrinck and Debrunner-Vossbrinck, 2005) are surrounded by rounded rectangles. Genus names belonging to taxa present in both phylogenies are highlighted in bold. Bootstrap values of maximum likelihood (ML) analyses (LG + I + Γ4 model of evolution) are shown first, followed by posterior probabilities of Bayesian analyses (GTR + I + Γ4 model of evolution) for the ssrDNA phylogeny (A), and PhyloBayes (CATLG + I + Γ4 model of evolution) for the alpha-beta tubulin phylogeny (B). Black circles indicate ML bootstrap values and Bayesian posterior probabilities of 100%. Scale bar corresponds to 0.2 substitutions per site. Asterisk indicates the taxon for which the position in tubulin and ssuDNA phylogenies differs greatly, most likely due to an erroneous submission.

For the genus *Agmasoma* Hazard and Oldacre 1975, development includes one sequence that produces octospores within SVs. Diplokaryotic meronts divide by binary fission. Uninucleate sporonts undergo meiosis to produce an eight nucleate stage, in which plasmatomy occurs via internal budding (multiple division by vacuolation) and gives rise to eight sporoblasts. The pansporoblast membrane segregates externally from the sporont envelope. Spores have anisofilar polar filaments. *Agmasoma* spp. parasitises shrimps of the family Penaeidae worldwide.

3.6.1. Features of *A. penaei* (Sprague, 1950) Hazard and Oldacre, 1975

Agmasoma penaei (Sprague, 1950) Hazard and Oldacre, 1975 is a synonym of *Thelohania penaei* Sprague 1950 (Sprague, 1950). Merogony and sporogony as described for the genus. Late multinucleate sporonts are limited by electron-dense envelopes and enclosed in a pansporoblast membrane; expanded episporontal spaces are filled with dense secretion. Uninucleate sporoblasts with vacuolated cytoplasm and 35–45 nm thick envelopes reside inside SVs filled with granular and tubular secretions. Pyriform spores measure 2.7–4.2 × 1.5–3.7 μm; occasional teratogenic spores (macrospores) measure 4.7–7.00 × 2.5–3.13 μm. A mature spore displays an anisofilar (2–3 + 4–6 coils) polar tube, bipartite polaroplast and large posterosome. A spore wall consists of an electron-translucent endospore (100–120 nm) and exospore (30–50 nm). SVs are subspherical, 7.0–10.49 × 5.5–9.40 μm and limited by a thin membrane. Lumens of SVs are electron-lucent, without tubular secretion. We include the ssrDNA sequence with the GenBank accession number KF549987 in the diagnosis of this species. The type host is *Litopenaeus setiferus* Linnaeus, 1767. The type locality is defined as the Gulf of Mexico, offshore from Plaquemines and Jefferson Parishes, Louisiana, USA. The site of infection is in the female gonads and nodules, presumably produced from hypertrophied phagocytes, overloaded with spores, surrounded by haemocyte layers.

3.6.2. Type material

As we were unable to identify the location of type material, we designate neotype material, which includes: (i) neosyntype slides with Trichrome and Giemsa-stained smears from infected tissues and with Methylene blue-stained thick sections, labelled "Ap-Ls_2012LA" (Nos. 01–22) deposited to the slide collection of the Institute of Plant Protection, St. Petersburg, Russia ("Dr. Issi's collection") and stored in the private collection of Y. Sokolova; (ii) TEM blocks of Epon–Araldite-embedded ovary tissues of shrimps infected with *A. penaei* (labelled "case12-053"; "case12-119") stored in the private collection of Y. Sokolova; (iii) EM images labelled 2012-06-08_Ap-Ls: 001-086 deposited to the database of the Core Microscopy Center of SVM, LSU, Baton Rouge, LA, USA; and (iv) frozen purified *A. penaei* spores and samples of DNA isolated from these spores, stored in the Core Microscopy Center, SVM LSU, Baton Rouge LA, USA and in the laboratory of Nicolas Corradi at the Canadian Institute for Advanced Research, Department of Biology, University of Ottawa, Canada.

4. Discussion

The Louisiana, Thailand and Senegal isolates of *A. penaei* demonstrated similar morphology of spores and stages of intracellular development. All three isolates produce octets of pyriform mononucleate spores. The anisofilar polar filament with a straight manubrial part and a coiled region composed of two to three broad anterior and four to six narrow posterior coils, is a synapomorphy shared by all *A. penaei* isolates, which differentiates the genus *Agmasoma* from other octosporogenic *Thelohania*-like genera (Hazard and Oldacre, 1975). Despite structural similarity, the average size and proportions of spores reported for the Senegal isolate (4.7 × 2.9 μm, length-to-width ratio (l/w) = 1.6 (Clotilde-Ba and Toguebaye, 1994) differed significantly from the Louisiana (3.7 × 2.1 μm, l/w = 1.8) (herein) and the Thailand (3.6 × 2.1 μm, l/w = 1.7) (Laisutisan et al., 2009) isolates.

The information about ultrastructure of pre-spore stages of the Senegal and especially of the Thailand isolate is scarce, and only a few features can be compared properly. All three isolates definitely possess a diplokaryotic stage at the onset of sporogony and share the same mode of sporont division – i.e. "not by budding, but

instead, by a delayed aggregation of protoplasm after three nuclear divisions to form eight spores" (Hazard and Oldacre, 1975). In all three *A. penaei* isolates, segregation of individual sporoblasts occurs within a sporont at the eight-nucleate stage.

The records on the tissue tropism of *A. penaei* are extremely inconsistent (Table 1). For example, the *A. penaei*–Thai isolate was recorded from abdominal muscles and hepatopancreas of the Pacific white shrimp *L. vannamei*, whereas the Senegal isolate infected many tissues including heart musculature, nervous system and gonads of *F. notialis* and displayed no tissue specificity at all. Our data confirm that gonads are the primary site of *A. penaei* infection in the type host *L. setiferus* in the type locality, Louisiana coast of the Gulf of Mexico, as it was stated in the original description of the microsporidium (Sprague, 1950; Hazard and Oldacre, 1975). The subcuticular masses of spores, 10–500 nm in diameter, surrounded by haemocyte layers, probably result from encapsulation of pieces of infected tissues, a common defense reaction against foreign material in arthropods. Smaller nodule-like formations could be phagocytes loaded with spores, similar to giant cells described recently in *A. rohanae* (Stentiford et al., 2014). We never observed large "xenoma"-type cysts in muscles, such as those reported in *F. notialis* infected with the Senegal isolate of *A. penaei* (Clotilde-Ba and Toguebaye, 1994).

Such flexible tissue tropism appears very improbable for one and the same microsporidium species and may result from misidentification of either the tissues or the parasite species. Our experience suggests that identification of the tissue of parasite localisation in an infected shrimp is not easy. The infected gonads are hypertrophied and modified, and spores contaminate all tissues when isolated from the infected shrimp. We were able to unequivocally determine the tissues of parasite localisation only in histological sections stained with Luna stain (Peterson et al., 2011). Moreover, infection of the same shrimp with two or three species of microsporidia is not unusual (Overstreet, 1973), and some records of multiple tissue tropism might be attributed to the overlooked double infection. For example, during examination of *A. penaei*-infected shrimps for this paper, we found that muscle of two examined animals were co-infected with *Perezia nelsoni* (Y. Sokolova and J. Hawke, unpublished observations).

The ssrDNA sequence variations (Fig. 7), as well as the estimated evolutionary distance between two geographical isolates, suggest that these should rather be considered as separate species. Indeed, pairwise sequence divergence between the ssrRNA gene of *A. penaei* isolated from infected shrimp in the Gulf of Mexico and an orthologue sequence from the Thailand isolate was 0.066, which is higher than typically recorded intraspecific differences. Comparable or lesser divergence was observed between congeners. Divergence between ssrDNA sequences of *A. michaelis* and *Ameson pulvis* or *Nadelspora canceri* (presumably one dimorphic species (Stentiford et al., 2013a)) was 0.088, and it was as low as 0.004 between ssrDNA genes of *Hamiltosporidium tvaerminnensis* and *Hamiltosporidium magnivora*. Moreover, evolutionary distances comparable with those separating two *A. penaei* isolates were found between representatives of different genera: 0.055 between *G. anomala* and *H. anguillarum* and 0.083 between *N. salmonis* and *D. lepeophtherii* (Table 3). In the literature, ssrDNA sequences of microsporidia display pairwise distances among congeners ranging from 0.01–0.04 for *Liebermannia* spp. (Sokolova et al., 2009), 0.01–0.09 for *Amblyospora* spp. (Baker et al., 1998), 0.01–0.05 for *Paranosema* spp. (Sokolova et al., 2003), 0.01–0.03 for *Nosema–Vairimorpha* spp. from Lepidoptera (Baker et al., 1994), and 0.03–0.10 for *Encephalitozoon* spp. (Lange et al., 2009).

It should be also mentioned here that molecular (Pasharawipas et al., 1994) and morphological characterisation (Laisutisan et al., 2009) of the Thailand isolate of *A. penaei* were performed 15 years apart using different host species (*L. vannamei* and *P. monodon*), so it cannot be excluded that two different forms (strains or species) had been studied in Thailand.

The Senegal isolate can be differentiated from both Louisiana and Thailand isolates by spore proportions and the ability to produce xenomas, and probably also represents a separate species. Until more information regarding the ultrastructure and genomics of these and other strains isolated worldwide is available, we can only speculate that *A. penaei* represents a cline of highly related forms, gradually diversifying within penaeid crustaceans over geographical space and time.

During the unique sporogony of *A. penaei*, regions of the cytoplasm surrounding sporont nuclei are isolated from each other by flattened membrane profiles filled with electron-dense material produced de novo within the sporont cytoplasm (herein; Clotilde-Ba and Toguebaye, 1994). In addition, the envelope of SVs enclosing spore octets at the end of sporogony originates from the membranous envelope of the eight-nucleate sporont (herein; Clotilde-Ba and Toguebaye, 1994). Among microsporidia, a similar type of division, termed multiple division by vacuolisation or internal budding, has been recorded only for two presumably basal groups of microsporidia, metchnikovellids and chytriopsids, as a part of their sac-bound sporogony (Larsson and Køie, 2006; Sokolova et al., 2014). Similar to sac-bound sporonts of metchnikovellids, *A. penaei* sporonts contained characteristic roundish vacuoles 200–500 nm in diameter with electron-dense cores, membrane whorls and other membrane structures (Fig. 5B). In metchnikovellids, however, the whole sporont envelope transforms into a thick cyst wall, whereas in *Agmasoma* only a thin submembrane layer of the sporont plasmalemma becomes a SV membrane. The rest of the membrane thickens to become the wall of the sporoblast mother cell (the late sporont), which gives rise to sporoblasts. A significant part of this wall seems to disintegrate during sporulation; in all three isolates studied ultrastructurally, numerous wall fragment-like inclusions, observed within SVs with sporoblasts and young spores, disappeared upon spore maturation (Clotilde-Ba and Toguebaye, 1994; Laisutisan et al., 2009; herein). *Agmasoma* development demonstrates that internal budding is not necessarily coupled with cyst-bound sporogony and might be more widely distributed among microsporidia than has been previously thought.

The karyogamy of the diplokaryon counterparts and the presence of synaptonemal complexes (chromosome bivalents in diakinesis) at the onset of sporogony, indicative of meiosis, followed by three consecutive divisions to produce an octet of spores, are the basal life-cycle features of microsporidia, probably inherited from a sexual microsporidian-fungal ancestor (Lee et al., 2008; James et al., 2013), and later eliminated in more derived microsporidian genera such as *Nosema*, *Encephalitozoon*, *Enterocytozoon* and others.

The anisofilar polar filament, with its broad and narrow parts homologous to the manubrium and manubrial cisternae of metchnikovellids (Sokolova et al., 2013), could also be an ancestral feature.

Another plesiomorphic feature may be a polyxenous life-cycle (Vossbrinck and Debrunner-Vossbrinck, 2005), and the presence of an intermediate host in the life cycle of *A. penaei* has been suggested by several authors (see below).

White Atlantic shrimp *L. setiferus* and other seven host species listed for *A. penaei* (Table 1) all belong to the family Penaeidae. This family represents the suborder Dendrobranchiata and occupies the basal position on the phylogenetic tree of Decapoda (Porter et al., 2005). The second suborder Polyciemata, a sister taxon to Dendrobranchiata, unites seven other groups (infraorders) of extant decapods (Porter et al., 2005; De Grave et al., 2009). Among the 17 genera of microsporidia recorded from decapods, representatives of four genera (*Tuzetia*, *Perezia*, *Enterocytozoon* and *Agmasoma*) are found in penaeid shrimps. The species of the other 13 genera are distributed among four infraorders: Astacidea (crayfish and

lobsters, three genera), Anomura (hermit and snow crabs, two genera), Caridea (shrimps, three genera), and Brachiura (crabs, five genera) (Canning et al., 2002; Stentiford et al., 2013b, 2014). High divergence of ssrRNA and tubulin genes of *A. penaei* and the basal position of *A. penaei* within the *Endoreticulatus–Vittaforma–Agmasoma* lineage may reflect a long eco-evolutionary history of this species with Penaeidae.

Our phylogenetic analyses using tubulin- and small subunit gene sequences consistently placed *A. penaei* in the lineage corresponding to the "Clade IV of microsporidia of terrestrial origin" (Vossbrinck and Debrunner-Vossbrinck, 2005) (Figs. 8 and 9), together with parasites of brine shrimp, cladocerans and free living copepods inhabiting fresh and salt water inland reservoirs.

The length of the *A. penaei* branch, as well as the scarcity of taxa on the tubulin tree, might be responsible for inconsistency in the position of *A. penaei* within Clade IV: in small subunit phylogeny *A. penaei* clusters with the *Vittaforma–Endoreticulatus* branch, although with low statistical support; whilst in alpha- and beta-tubulin phylogeny it clusters with *Enterocytozoon bieneusi*. Two microsporidia belonging to distantly related genera, namely *Endoreticulatus* sp. Zhenjiang and *Nosema bombycis*, unexpectedly formed a dichotomy on the tubulin tree, likely due to an erroneous submission.

Clustering of *A. penaei* with microsporidia of terrestrial origin parasitising crustaceans unrelated to penaeids and other groups of hosts also raises ecological considerations. The host of *A. penaei*, *L. setiferus*, plays an exceptional role in the ecology of the Gulf of Mexico coastal waters, being in the intersection of major food chains. The lifespan of this shrimp contains larval and early post-larval plankton stages inhabiting river estuaries with low salinity (0.2–10 ppt) and feeding on algae, insect larvae and small crustaceans, while juveniles and adults are benthic dwellers migrating far off shore in higher salinity (>35 ppt) sea waters, feeding predominantly on faecal pellets of fish and invertebrates and becoming, in turn, prey for those (Perez Farfante, 1969; Muncy, 1984). The life cycle, which includes inhabiting various niches during the life time, is typical for all extant species of penaeid shrimp and most likely was also characteristic for their ancestor. Such a lifestyle may have facilitated numerous host switches in the early stages of *Agmasoma* evolution, i.e. infection could easily be passed from (to) the shrimp to (from) an aquatic insect larvae, fresh/brackish water copepod or a fish. As a result, hosts with complicated lifestyles and diverse food habits, such as shrimp or crabs, could play a key role in the diversification of microsporidia, spreading the parasites along diverse food chains among terrestrial, freshwater and marine hosts, and perhaps establishing some of the contemporary host–parasite associations.

The routes of transmission and circulation of *A. penaei* in marine ecosystems remain completely unknown. Given the observed infection of female gonads, it may be presumed that light or benign infection could contribute to transovarial (vertical) transmission. However, infections of gonads observed during this study as well as by previous authors (Overstreet, 1973; Kelly, 1979) were always extremely severe and could lead to complete castrations. Numerous attempts to per-orally infect shrimp with the microsporidium always failed, and it was hypothesised and supported by a series of circumstantial evidence (Overstreet, 1973; Johnson, 1995), including application of *A. penaei*-specific DNA probes (Pasharawipas and Flegel, 1994), that transmission of *A. penaei* involves an intermediate host, presumably a perciform fish. Thus another player, a fish host, might be involved in *A. penaei–L. setiferus* interactions, and further studies of this host–parasite system could bring new insights in uncovering complex ecological bonds within a vulnerable Gulf of Mexico biota, vital for sustainable shrimp fishery.

The present study also paves the way for future studies based on whole genome analyses, using *A. penaei* as a model. Indeed, this species produces a large amount of spores that are easy to collect and clean, and is thus highly amenable to DNA extraction and next generation sequencing procedures. To this end, genome sequencing of this species is presently ongoing and we hope this will result in outstanding insights into mechanisms and tools that *A. penaei* uses to infect the White Atlantic shrimp. Moreover, this genome sequencing effort may unravel the presence of many genes that may have resulted from a long-term co-evolution between those species including horizontal gene transfers, and those involved in the dialogue between *A. penaeia* and the shrimp (i.e. effectors and other secreted genes; reviewed in Corradi and Selman, 2013).

Acknowledgements

We acknowledge the Microscopy Core Center of Louisiana State University School of Veterinary Medicine, USA and funding from Louisiana Department of Wildlife and Fisheries, USA. We thank Nicolas George (Louisiana State University) for assistance in EM, and two anonymous reviewers whose suggestions improved the paper. Nicolas Corradi is a fellow of the Canadian Institute for Advanced research, and his work is supported by Discovery Grants from the Natural Sciences and Engineering Research Council of Canada. We thank Martin Bourgeois, Marine Biologist, Louisiana Department of Wildlife and Fisheries and Albert "Rusty" Gaude, Area Agent of the LSU AgCenter, for information concerning the occurrence of diseased shrimp and submission of specimens examined in this study.

Appendix A. Supplementary data

Supplementary data associated with this article can be found, in the online version, at http://dx.doi.org/10.1016/j.ijpara.2014.07.013.

References

Altschul, S.F., Koonin, E.V., 1998. Iterated profile searches with PSI-BLAST – a tool for discovery in protein databases. Trends Biochem. Sci. 23, 444–447.

Baker, M.D., Vossbrinck, C.R., Becnel, J.J., Andreadis, T.G., 1998. Phylogeny of *Amblyospora* (Microsporida: Amblyosporidae) and related genera based on small subunit ribosomal DNA data: a possible example of host parasite cospeciation. J. Invertebr. Pathol. 71, 199–206.

Baker, M.D., Vossbrinck, C.R., Maddox, J.V., Undeen, A.H., 1994. Phylogenetic relationships among *Vairimorpha* and *Nosema* species (Microspora) based on ribosomal RNA sequence data. J. Invertebr. Pathol. 64, 100–106.

Bell, T.A., Lightner, D.V., 1988. A Handbook of Normal Penaeid Shrimp Histology. World Aquaculture Society, Baton Rouge, LA.

Canning, E.U., Curry, A., Overstreet, R.M., 2002. Ultrastructure of *Tuzetia weidneri* sp. n. (Microsporidia: Tuzetiidae) in skeletal muscle of *Litopenaeus setiferus* and *Farfantepenaeus aztecus* (Crustacea: Decapoda) and new data on *Perezia nelsoni* (Microsporidia: Pereziidae) in *L. setiferus*. Acta Protozool. 41, 63–77.

Clotilde-Ba, F.L., Toguebaye, B.S., 1994. Ultrastructure and development of *Agmasoma penaei* (Microspora, Thelohaniidae) found in *Penaeus notialis* (Crustacea, Decapoda, Penaeidae) from Senegal. Eur. J. Protistol. 30, 347–353.

Clotilde-Ba, F.L., Toguebaye, B.S., 2001. Infection of *Penaeus monodon* (Fabricius, 1798) (Crustacea, Decapoda, Penaeidae) by *Agmasoma penaei* (Microspora, Thelohaniidae) in Senegal, West Africa. Bull. Eur. Assoc. Fish Pathol. 21, 157–159.

Corradi, N., Haag, K.L., Pombert, J.F., Ebert, D., Keeling, P.J., 2009. Draft genome sequence of the *Daphnia* pathogen *Octosporea bayeri*: insights into the gene content of a large microsporidian genome and a model for host–parasite interactions. Genome Biol. 10.

Corradi, N., Selman, M., 2013. Latest progress in microsporidian genome research. J. Eukaryot. Microbiol. 60, 309–3012.

Corsaro, D., Walochnik, J., Venditti, D., Steinmann, J., Müller, K.-D., Michel, R., 2014. Microsporidia-like parasites of amoebae belong to the early fungal lineage Rozellomycota. Parasitol. Res. 113, 1909–1918.

Darriba, D., Taboada, G.L., Doallo, R., Posada, D., 2011. ProtTest 3: fast selection of best-fit models of protein evolution. Bioinformatics 27, 1164–1165.

De Grave, S., Pentcheff, N.D., Ahyong, S.T., Chan, T.-Y., Crandall, K.A., Dworcshak, P.C., Felder, D.L., Feldman, R.M., Fransen, C.H., Goulding, L.Y., Lemaitre, R., Low, M.E., Martin, J.W., Ng, R.K., Schweltzer, C.E., Tan, S.H., Tshudy, D., Wetzer, R., 2009. A classification of living and fossil genera of decapod crustaceans. Raffles Bull. Zool., 1–109.

Edgar, R.C., 2004. MUSCLE: multiple sequence alignment with high accuracy and high throughput. Nucleic Acids Res. 32, 1792–1797.
Flegel, T.W., Flegan, D.F., Kongsom, S., Vuthikornudomikit, S., Sriurairatana, S., Boonyaratpalin, S., Chantanachookin, C., Vickers, J., MacDonald, O., 1992. Occurence, diagnosis and treatment of shrimp diseases in Thailand. In: Fulks, W., Main, K. (Eds.), Diseases in Cultured Penaeid Shrimp in Asia and the United States. The Oceanic Institute, Honolulu, HI, pp. 57–112.
Gunter, G., 1967. Some relationships of estuaries to the fisheries of the Gulf of Mexico. In: Lauff, G.A. (Ed.), Estuaries. Am. Assoc. Adv. Sci., Washington, DC, pp. 621–638.
Hazard, E.I., Oldacre, S.W., 1975. Revision of Microsporida (Protozoa) close to *Thelohania*: with description of one new family, eight new genera, and thirteen new species. Tech. Bull. USDA No. 1530. Agricultural Research Service, pp. 1–104.
Hutton, R.F., Sogandares-Bernal, F., Ingles, R.M., Woodburn, K.D., 1959. Investigations on the parasite and diseases of saltwater shrimps (Penaeidae) of sports and commercial importance in Florida. Florida Board Conservation Marine Laboratory Technical Series.
James, T.Y., Pelin, A., Bonen, L., Ahrendt, S., Sain, D., Corradi, N., Stajich, J.E., 2013. Shared signatures of parasitism and phylogenomics unite Cryptomycota and Microsporidia. Curr. Biol. 23, 1548–1553.
Johnson, S.K., 1995. Handbook of Shrimp Diseases. Department of Wildlife and Fishery Sciences Texas A&M University Series, College Station, TX, USA.
Jones, S.R.M., Prosperi-Porta, G., Kim, E., 2012. The diversity of microsporidia in parasitic copepods (Caligidae: Siphonostomatoida) in the northeast Pacific Ocean with description of *Facilispora margolisi* n. g., n. sp. and a new family Facilisporidae n. fam. J. Eukaryot. Microbiol. 59, 206–217.
Kelly, J.F., 1979. Tissue specificities of *Thelohania duorara, Agmasoma penae*i, and *Pleistophora* sp., microsporidian parasites of pink shrimp, *Penaeus duorarum*. J. Invertebr. Pathol. 33, 331–339.
Laisutisan, K., Prasertsri, S., Chuchird, N., Limsuwan, C., 2009. Ultrastructure of the microsporidian *Thelohania (Agmasoma) penae*i in the pacific white shrimp (*Litopenaeus vannamei*). Kasetsart J. Nat. Sci. 33, 41–48.
Lange, C.E., Johny, S., Baker, M.D., Whitman, D.W., Solter, L.F., 2009. A new *Encephalitozoon* species (Microsporidia) isolated from the lubber grasshopper, *Romalea microptera* (Beauvois) (Orthoptera: Romaleidae). J. Parasitol. 95, 976–986.
Larsson, R., Køie, M., 2006. The ultrastructure and reproduction of *Amphiamblys capitellides* (Microspora, Metchnikovellidae), a parasite of the gregarine *Ancora sagittata* (Apicomplexa, Lecudinidae), with redescription of the species and comments on the taxonomy. Eur. J. Protistol. 42, 233–248.
Lartillot, N., Lepage, T., Blanquart, S., 2009. PhyloBayes 3: a Bayesian software package for phylogenetic reconstruction and molecular dating. Bioinformatics 25, 2286–2288.
Lee, S.C., Corradi, N., Byrnes Iii, E.J., Torres-Martinez, S., Dietrich, F.S., Keeling, P.J., Heitman, J., 2008. Microsporidia evolved from ancestral sexual fungi. Curr. Biol. 18, 1675–1679.
Lightner, D.V., 1996. A Handbook of Pathology and Diagnostic Procedures for Diseases of Cultured Penaeid Shrimp. World Aquaculture Society, Baton Rouge, LA.
Luna, L.G., 1968. Manual of Histologic Staining Methods of the Armed Forces Institute of Pathology. The Armed Forces Institute of Pathology, McGraw-Hill, New York.
Miglarese, J.V., Shealy, M.H., 1974. Incidence of microsporidia and trypanorhynch cestodes in white shrimp, *Penaeus setiferus* Linnaeus in South Carolina estuaries. Bull. South. Calif. Acad. Sci. 36, 93.
Morado, J.F., 2011. Protistan diseases of commercially important crabs: a review. J. Invertebr. Pathol. 106, 27–53.
Muncy, R.J., 1984. Species Profiles: Life Histories and Environmental Requirements of Coastal Fishes and Invertebrates (South Atlantic): White Shrimp. U.S. Fish and Wildlife Service FWS/OBS-82/11.27. U.S. Army Corps of Engineers, TR EL-82-4. <http://www.sms.si.edu/irlspec/Penaeu_setife>.
Nei, M., Kumar, S., 2000. Molecular Evolution and Phylogenetics. Oxford University Press, New York.
Overstreet, R.M., 1973. Parasites of some penaeid shrimps with emphasis on reared hosts. Aquaculture 1, 105–140.
Pasharawipas, T., Flegel, T.W., 1994. A specific DNA probe to identify the intermediate host of a common microsporidian parasite of *Penaeus merguensis* and *P. monodon*. Asian Fish Sci. 7, 157–167.
Pasharawipas, T., Flegel, T.W., Chaiyaroj, S., Mongkolsuk, S., Sirisinha, S., 1994. Comparison of amplified RNA gene sequences from microsporidian isolates (*Agmasoma* or *Thelohania*) in *Penaeus merguensis* and *P. monodon*. Asian Fish Sci. 7, 169–178.
Perez Farfante, I., 1969. Western Atlantic shrimps of the genus *Penaeus*. Fish. Bull. 67, 461–591.
Perez Farfante, I., 1997. Penaeoid and sergestoid shrimps and prawn of the world. Keys and diagnoses for the families and genera. Mem. Mus. Natl. Hist. Nat. 175, 1–233.
Peterson, T.S., Spitsbergen, J.M., Feist, S.W., Kent, M.L., 2011. Luna stain, an improved selective stain for detection of microsporidian spores in histologic sections. Dis. Aquatic Org. 95, 175–180.
Porter, M.L., Pérez-Losada, M., Crandall, K.A., 2005. Model-based multi-locus estimation of decapod phylogeny and divergence times. Mol. Phylogenet. Evol. 37, 355–369.
Rode, N.O., Landes, J., Lievens, E.J.P., Flaven, E., Segard, A., Jabbour-Zahab, R., Michalakis, Y., Agnew, P., Vivarès, C.P., Lenormand, T., 2013. Cytological, molecular and life cycle characterization of *Anostracospora rigaudi* n. g., n. sp. and *Enterocytospora artemiae* n. g., n. sp., two new microsporidian parasites infecting gut tissues of the brine shrimp *Artemia*. Parasitology 140, 1168–1185.
Ronquist, F., Teslenko, M., Van Der Mark, P., Ayres, D.L., Darling, A., Höhna, S., Larget, B., Liu, L., Suchard, M.A., Huelsenbeck, J.P., 2012. Mrbayes 3.2: efficient bayesian phylogenetic inference and model choice across a large model space. Syst. Biol. 61, 539–542.
Sokolova, Y.Y., Dolgikh, V.V., Morzhina, E.V., Nassonova, E.S., Issi, I.V., Terry, R.S., Ironside, J.E., Smith, J.E., Vossbrinck, C.R., 2003. Establishment of the new genus *Paranosema* based on the ultrastructure and molecular phylogeny of the type species *Paranosema grylli* gen. nov., comb. nov (Sokolova, Selezniov, Dolgikh, Issi 1994), from the cricket *Gryllus bimaculatus* Deg. J. Invertebr. Pathol. 84, 159–172.
Sokolova, Y.Y., Fuxa, J.R., 2008. Biology and life-cycle of the microsporidium *Kneallhazia solenopsae* Knell Allan Hazard 1977 gen. n., comb. n., from the fire ant *Solenopsis invicta*. Parasitology 135, 903–929.
Sokolova, Y.Y., Lange, C.E., Mariottini, Y., Fuxa, J.R., 2009. Morphology and taxonomy of the microsporidium *Liebermannia covasacrae* n. sp. from the grasshopper *Covasacris pallidinota* (Orthoptera, Acrididae). J. Invertebr. Pathol. 101, 34–42.
Sokolova, Y.Y., Paskerova, G.G., Rotari, Y.M., Nassonova, E.S., Smirnov, A.V., 2013. Fine structure of *Metchnikovella incurvata* Caullery and Mesnil 1914 (Microsporidia), a hyperparasite of gregarines *Polyrhabdina* sp. from the polychaete *Pygospio elegans*. Parasitology 140, 855–867.
Sokolova, Y.Y., Paskerova, G.G., Rotari, Y.M., Nassonova, E.S., Smirnov, A.V., 2014. Description of *Metchnikovella spiralis* sp.n. (Microsporidia:Metchnikovellidae), with notes on the ultrastructure of metchnikovellids. Parasitology 141, 1108–1122.
Sprague, V., 1950. Notes on Three Microsporidian Parasites of Decapod Crustacea of Louisiana Coastal Water. Occas. Pap. Mar. Lab. LA State Univ., Baton Rouge, LA, pp. 1–8.
Sprague, V., 1977. Annotated list of species of Microsporidia. In: Bulla, L.A., Cheng, T.C. (Eds.), Comparative Pathobiology, Systematics of the Microsporidia, vol. 2. Plenum Press, New York; London, pp. 31–334.
Sprague, V., Cough, J., 1971. An annotated list of protozoon parasites, hyperparasites and commensals of decapod crustacea. J. Protozool. 18, 526–537.
Stentiford, G.D., Bateman, K.S., Small, H.J., Moss, J., Shields, J.D., Reece, K.S., Tuck, I., 2010. *Myospora metanephrops* (n. g., n. sp.) from marine lobsters and a proposal for erection of a new order and family (Crustaceacida; Myosporidae) in the Class Marinosporidia (Phylum Microsporidia). Int. J. Parasitol. 40, 1433–1446.
Stentiford, G.D., Bateman, K.S., Feist, S.W., Chambers, E., Stone, D.M., 2013a. Plastic parasites: extreme dimorphism creates a taxonomic conundrum in the phylum Microsporidia. Int. J. Parasitol. 43, 339–352.
Stentiford, G.D., Feist, S.W., Stone, D.M., Bateman, K.S., Dunn, A.M., 2013b. Microsporidia: diverse, dynamic, and emergent pathogens in aquatic systems. Trends Parasitol. 29, 567–578.
Stentiford, G.D., Bateman, K.S., Feist, S.W., Oyarzun, S., Uribe, J.C., Palacios, M., Stone, D.M., 2014. *Areospora rohanae* n.gen. n.sp. (Microsporidia; Areosporiidae n. fam.) elicits multi-nucleate giant-cell formation in southern king crab (*Lithodes santolla*). J. Invertebr. Pathol. 118, 1–11.
Tamura, K., Peterson, D., Peterson, N., Stecher, G., Nei, M., Kumar, S., 2011. MEGA5: molecular evolutionary genetics analysis using maximum likelihood, evolutionary distance, and maximum parsimony methods. Mol. Biol. Evol. 28, 2731–2739.
Toubiana, M., Guelorget, O., Bouchereau, J.L., Lucien-Brun, H., Marques, A., 2004. Microsporidians in penaeid shrimp along the west coast of Madagascar. Dis. Aquatic Org. 58, 79–82.
Vidal-Martínez, V.M., Jiménez-Cueto, A.M., Simá-Álvarez, R., 2002. Parasites and symbionts of native and cultured shrimps from Yucatán, Mexico. J. Aquatic Anim. Health 14, 57–64.
Viosca, P., 1945. A critical analysis of practices in the management of warm-water fish with a view to greater food production. Trans. Am. Fisheries Soc. 73, 274–283.
Vossbrinck, C.R., Andreadis, T.G., Vavra, J., Becnel, J.J., 2004. Molecular phylogeny and evolution of mosquito parasitic microsporidia (Microsporidia: Amblyosporidae). J. Eukaryot. Microbiol. 51, 88–95.
Vossbrinck, C.R., Debrunner-Vossbrinck, B.A., 2005. Molecular phylogeny of the Microsporidia: ecological, ultrastructural and taxonomic considerations. Folia Parasitol. 52, 131–142.